Towards Laboratory Astrophysics In Plasma Wakefield Accelerators

Erwin Walter*
Max Planck Institute for Plasma Physics | Technical University of Munich
Munich, Germany

PhD Thesis Defense
January 2024

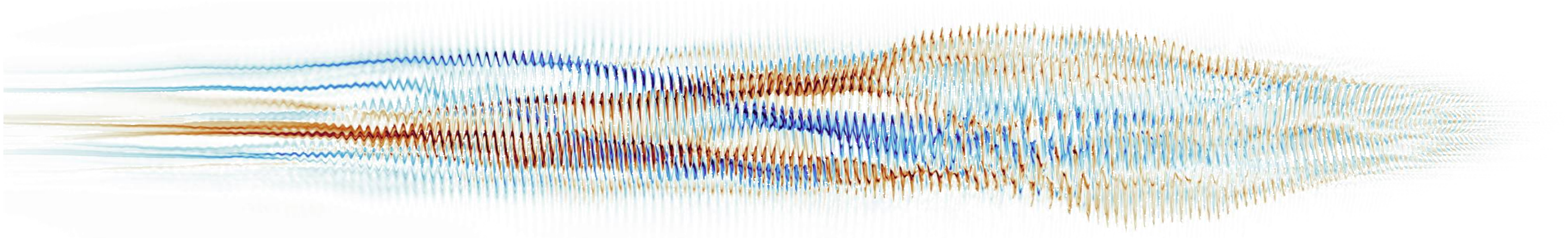

Advisor	John Farmer
Chair	Prof. Dr. Oliver Junge
1. Examiner	Hon.-Prof. Dr. Frank Jenko
2. Examiner	Prof. Dr. Eric Sonnendrücker

*Corresponding author:
erwinwalter11@web.de

Outline

Introduction and Contributions

Basics & Methods of Beam Plasma Physics

Laboratory-Relevant Filamentation Studies

- Analytical model for filamentation of cold and warm beams
- Application of the theory to experimental observation
- Beyond the model

Conclusion

Outline

Introduction and Contributions

Basics & Methods of Beam Plasma Physics

Laboratory-Relevant Filamentation Studies

- Analytical model for filamentation of cold and warm beams
- Application of the theory to experimental observation
- Beyond the model

Conclusion

PHYSICAL REVIEW E **110**, 035208 (2024)

Wakefield-driven filamentation of warm beams in plasma

Erwin Walter,[1,2,*] John P. Farmer,[3,†] Martin S. Weidl,[1] Alexander Pukhov,[4] and Frank Jenko[1]
[1]*TOK Department, Max Planck Institute for Plasma Physics, 85748 Garching, Germany*
[2]*Exzellenzcluster ORIGINS, 85748 Garching, Germany*
[3]*Future Accelerators Group, Max Planck Institute for Physics, 80805 Munich, Germany*
[4]*Institut für Theoretische Physik I, University of Duesseldorf, 40225 Duesseldorf, Germany*

(Received 12 June 2024; accepted 20 August 2024; published 19 September 2024)

PRE **Physical Review E** @PhysRevE · Sep 20
Wakefield-driven filamentation of warm beams in plasma, Erwin Walter, John P. Farmer, Martin S. Weidl, Alexander Pukhov, and Frank Jenko
@PlasmaphysikIPP go.aps.org/3Xwjkb4

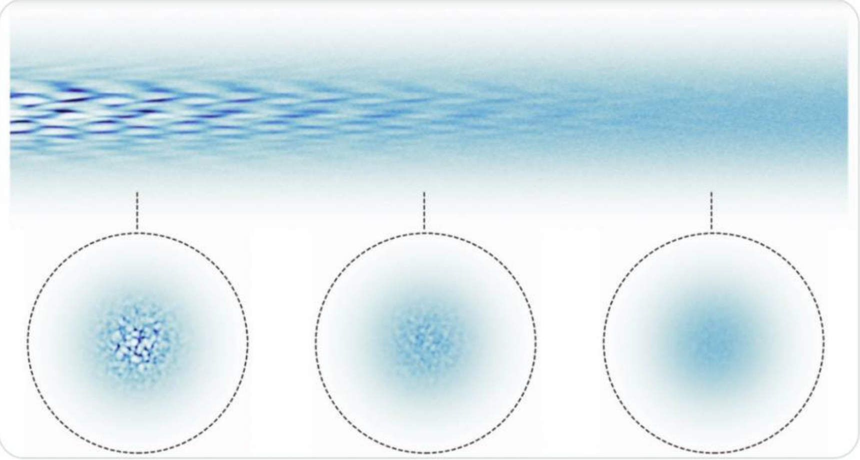

1 8 20 1.1K

Streams in Plasma

A particle stream in plasma is prone to **numerous filamentary instabilities**

- Kinetic energy → electromagnetic (EM) fluctuations
- Different regimes and effect of plasma ions

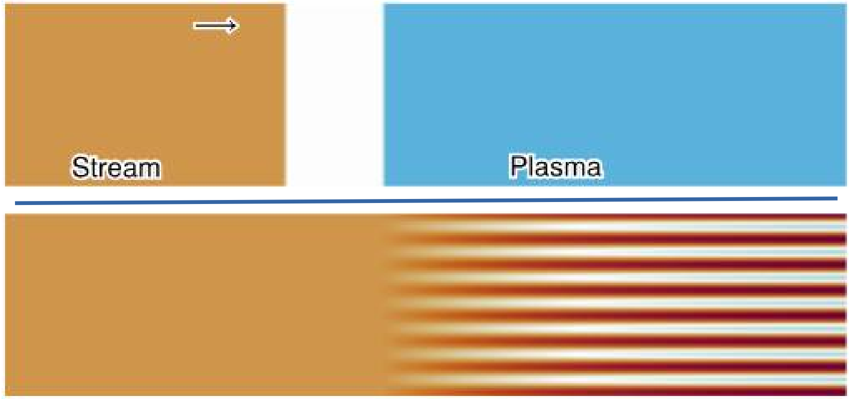

Streams in Plasma

A particle stream in plasma is prone to **numerous filamentary instabilities**

- Kinetic energy → electromagnetic (EM) fluctuations
- Different regimes and effect of plasma ions

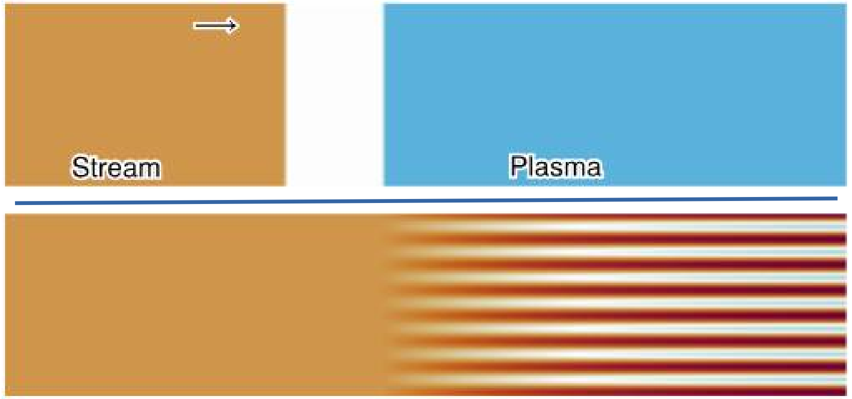

In astrophysical phenomena

- Possibly leading to collisionless shocks & particle acceleration

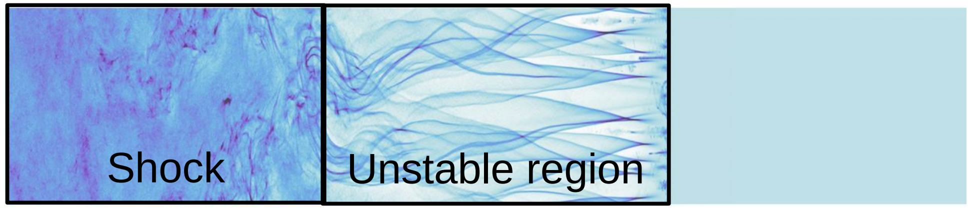

Streams in Plasma

A particle stream in plasma is prone to **numerous filamentary instabilities**

- Kinetic energy → electromagnetic (EM) fluctuations
- Different regimes and effect of plasma ions

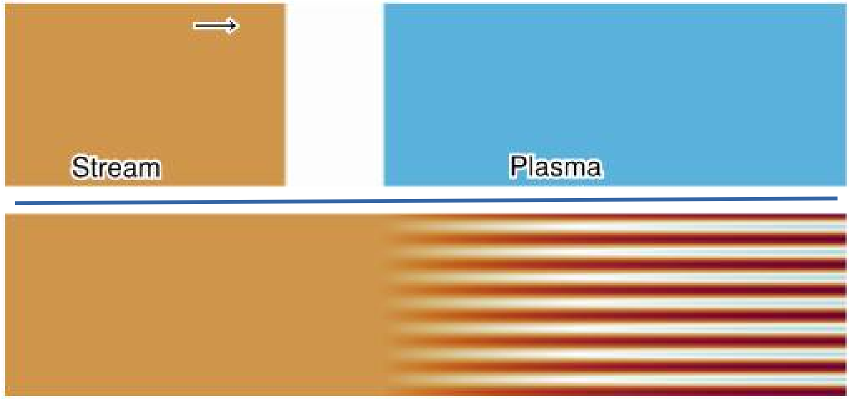

In astrophysical phenomena

- Possibly leading to collisionless shocks & particle acceleration

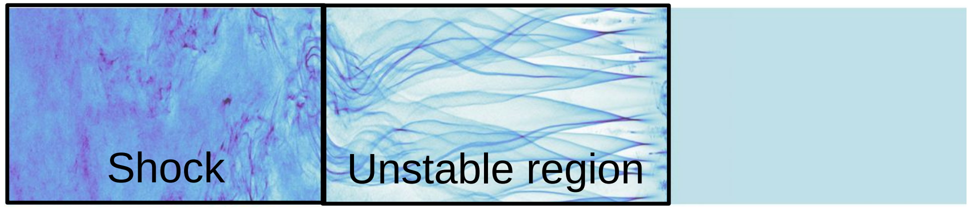

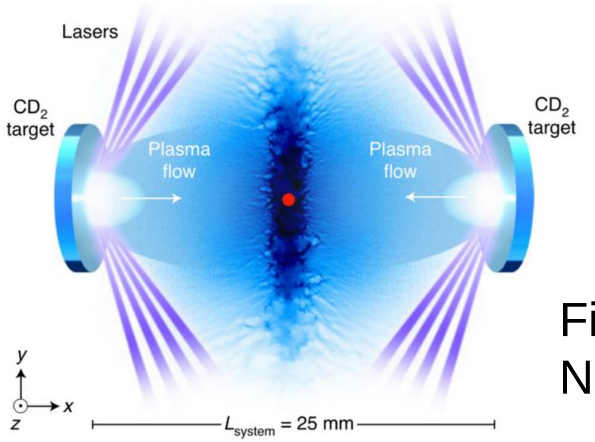

Fiuza *et al.*,
Nat. Phys., 2020

Streams in Plasma

A particle stream in plasma is prone to **numerous filamentary instabilities**

- Kinetic energy → electromagnetic (EM) fluctuations
- Different regimes and effect of plasma ions

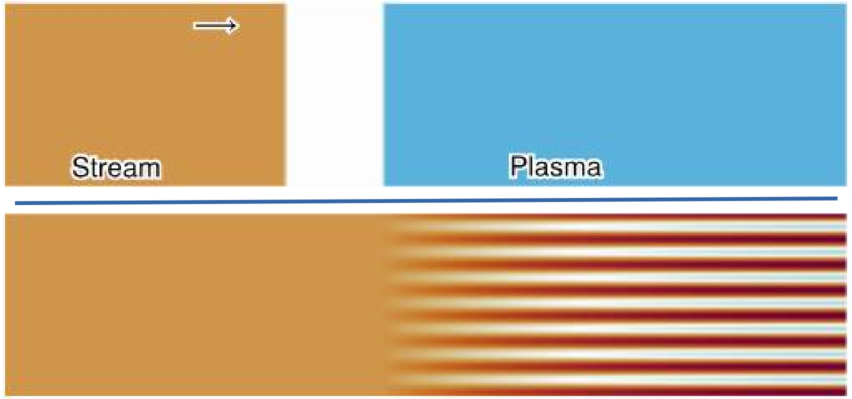

In astrophysical phenomena

- Possibly leading to collisionless shocks & particle acceleration

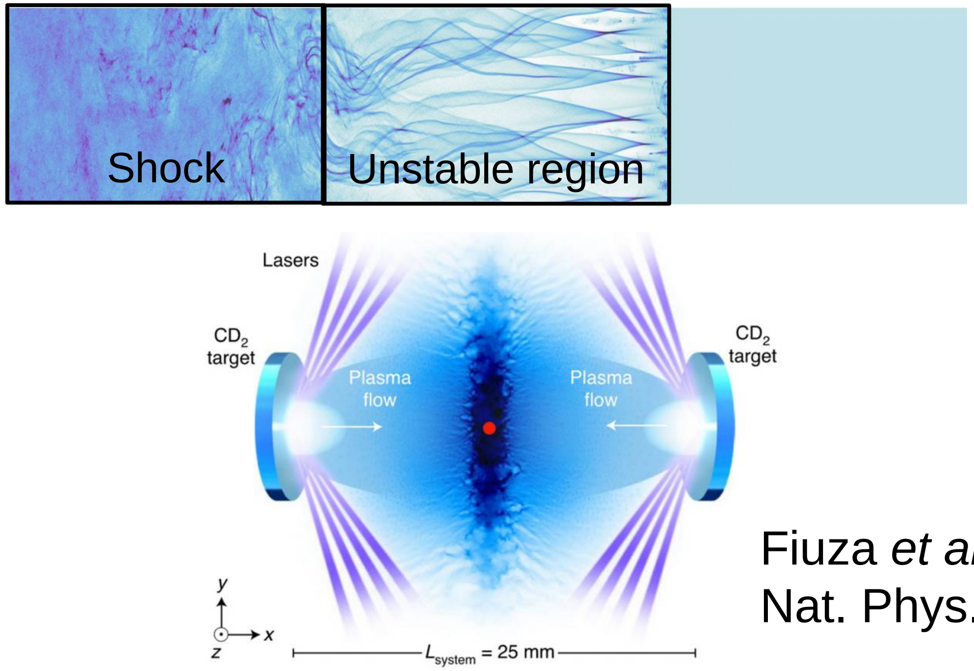

Fiuza *et al.*,
Nat. Phys., 2020

In plasma wakefield accelerators

- Avoided as accelerating field deteriorates

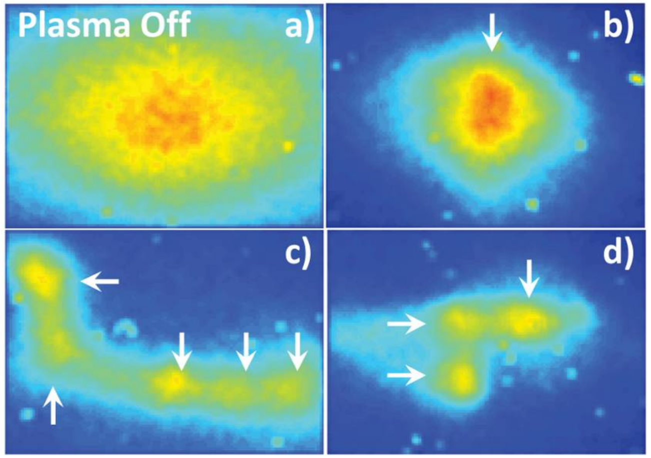

Allen *et al.*, PRL, 2012

Goal and Contributions of this Project

AWAKE possibly in different regime compared to previous works

- Beams with finite extent in astrophysical context and laboratory settings
- Previous analytical literature considers **non-bounded, homogeneous** streams

Goal and Contributions of this Project

AWAKE possibly in different regime compared to previous works

- Beams with finite extent in astrophysical context and laboratory settings
- Previous analytical literature considers **non-bounded, homogeneous** streams

Analytic model for laboratory-relevant filamentation instabilities
Walter, Farmer *et. al.,* Phys. Rev. E, 2024

- Comparison to particle-in-cell simulation and experimental observations
- Beyond the model

Goal and Contributions of this Project

AWAKE possibly in different regime compared to previous works

- Beams with finite extent in astrophysical context and laboratory settings
- Previous analytical literature considers **non-bounded, homogeneous** streams

Analytic model for laboratory-relevant filamentation instabilities

Walter, Farmer *et. al.,* Phys. Rev. E, 2024

- Comparison to particle-in-cell simulation and experimental observations
- Beyond the model

Application of numerical methods on beam-plasma studies

- Verification of different particle-in-cell methods for filamentation studies

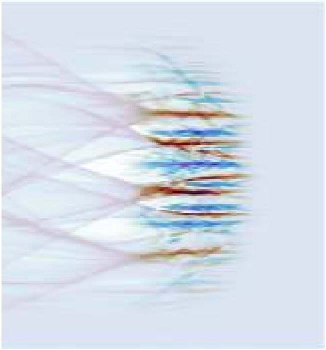

Goal and Contributions of this Project

DPS run enabled to study various gases with different atom mass

- The motion of plasma ions is usually neglected by choosing a high ion mass

Goal and Contributions of this Project

DPS run enabled to study various gases with different atom mass

- The motion of plasma ions is usually neglected by choosing a high ion mass

Effects of ion motion in wakefield-driven instabilities
Turner, Walter *et. al.* (AWAKE collab.), Phys. Rev. Lett.?, 2024

Density reduces towards beam tail
→ Self-modulated beam

Resurgent beam density

- Ion motion leads to suppression of the self-modulation

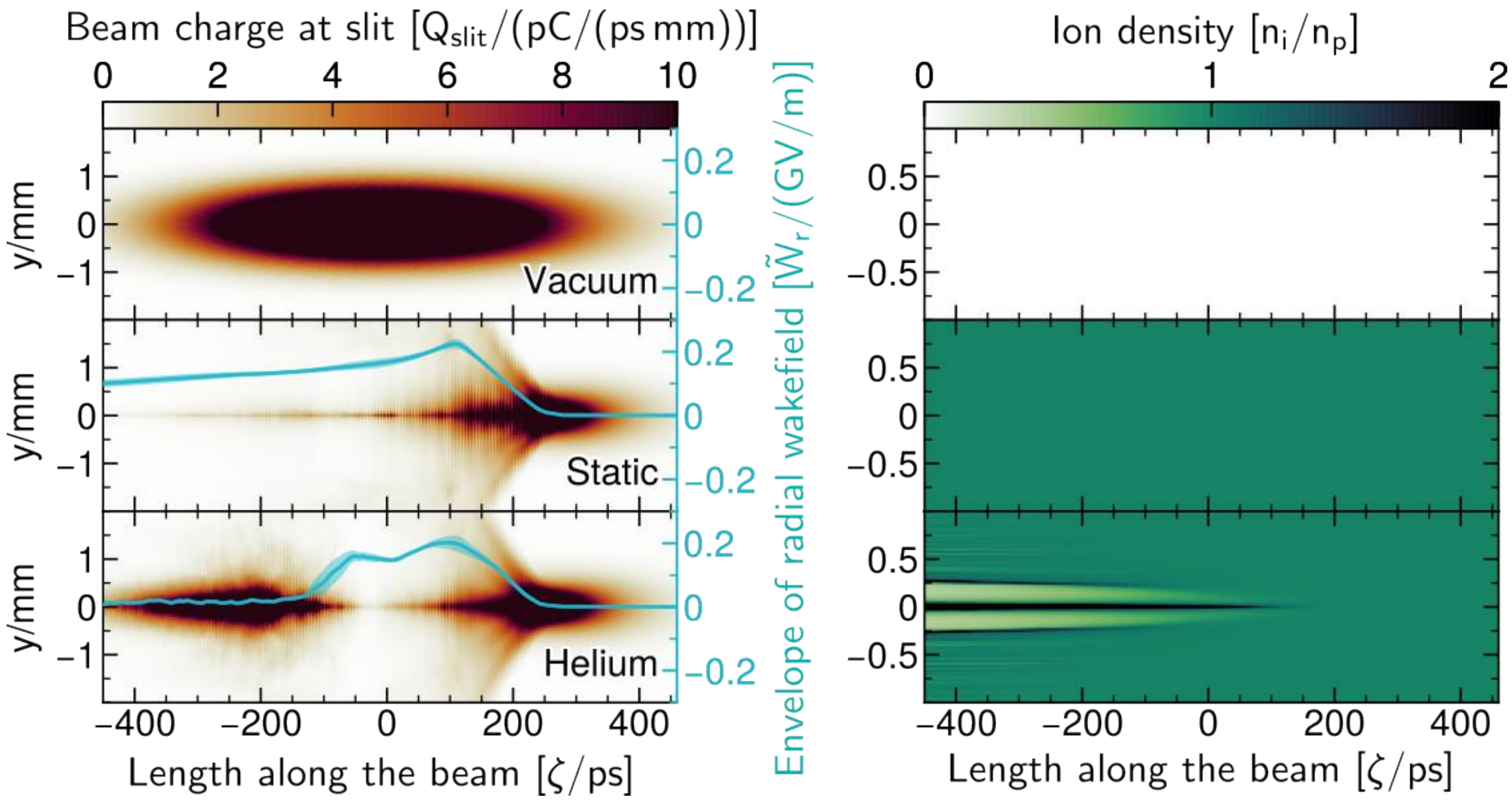

Filamentation Instabilities

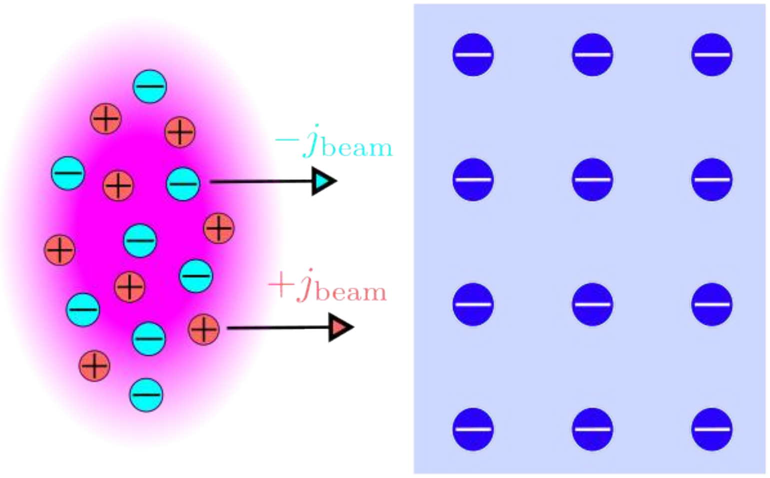

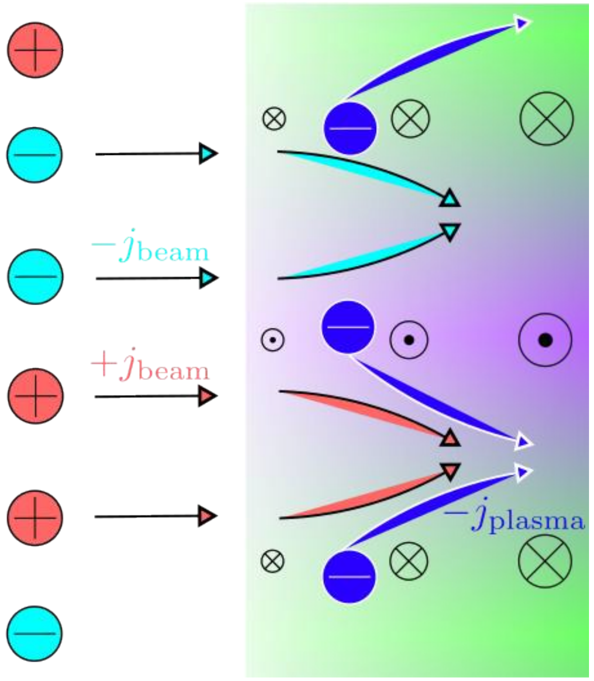

Current and charge fluctuation in particle stream excites small electromagnetic field

In plasma, the EM-field amplifies the transverse fluctuations within the stream

- Positive feedback

Filamentation Instabilities

Regimes for the filamentation instabilities are defined by the current imbalance

Bret *et al.*,
Phys. Rev. E,
2004

Filamentation Instabilities

Regimes for the filamentation instabilities are defined by the current imbalance

Bret *et al.*, Phys. Rev. E, 2004

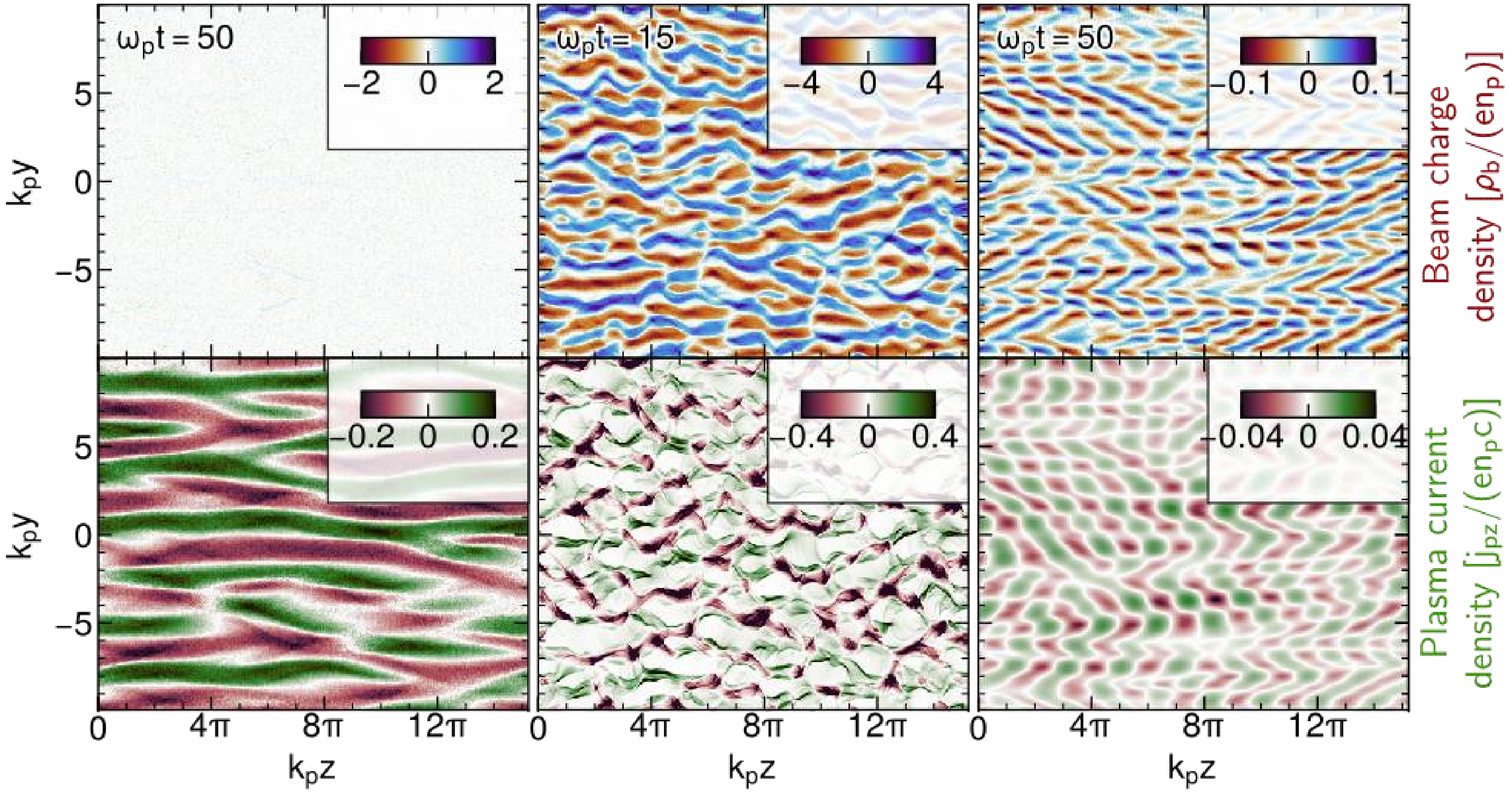

Symmetric system

Asymmetric system

Filamentation Instabilities

Regimes for the filamentation instabilities are defined by the current imbalance

Bret *et al.*, Phys. Rev. E, 2004

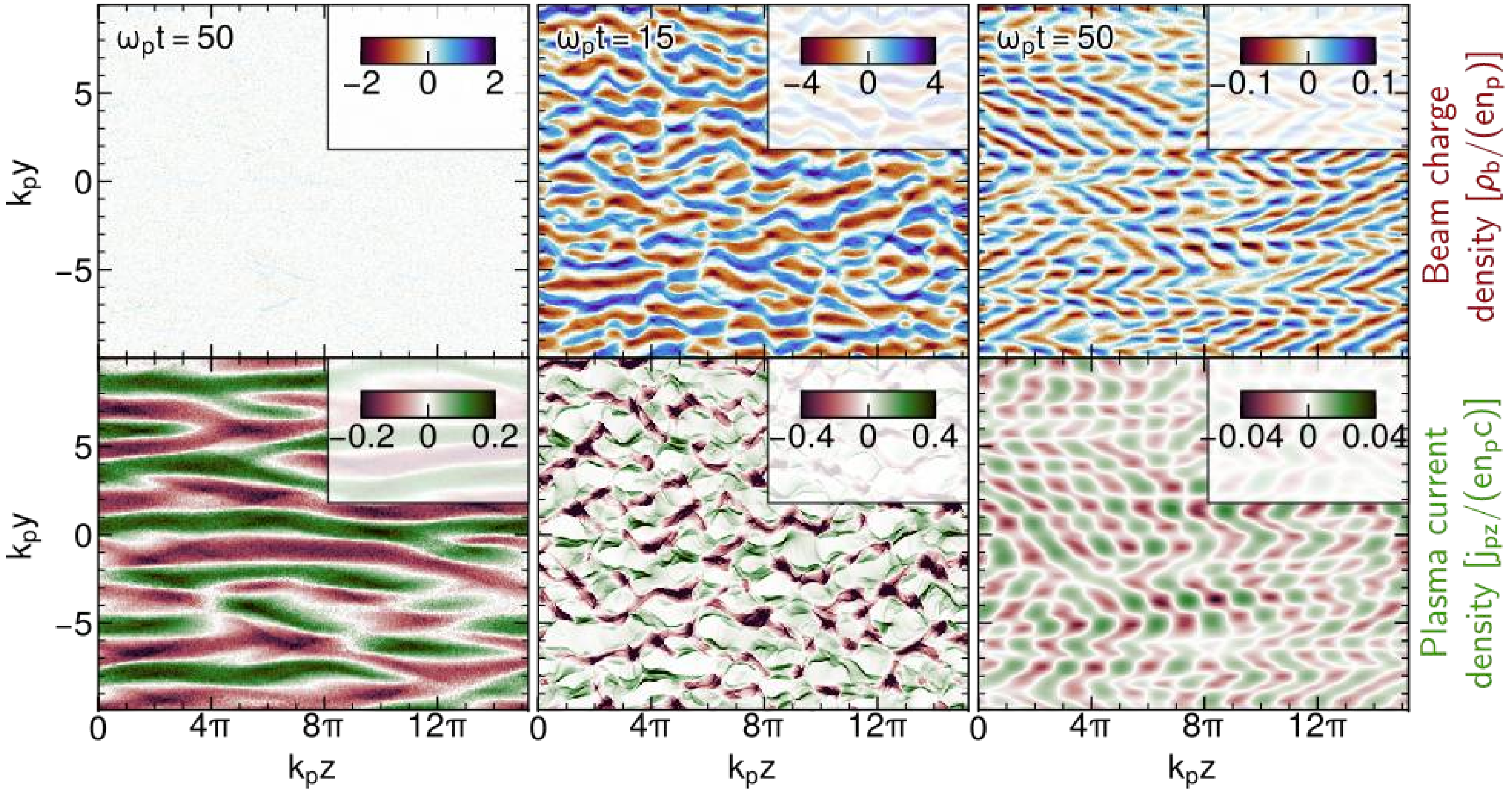

Symmetric system ⟷ Asymmetric system

Driven by plasma current/magnetic field | Driven by plasma oscillation/electric field

Transverse modulation | Longitudinal modulation

Structure

Introduction and Contributions

Basics & Methods of Beam Plasma Physics

Laboratory-Relevant Filamentation Studies

- Analytical model for filamentation of cold and warm beams
- Application of the theory to experimental observation
- Beyond the model

Conclusion

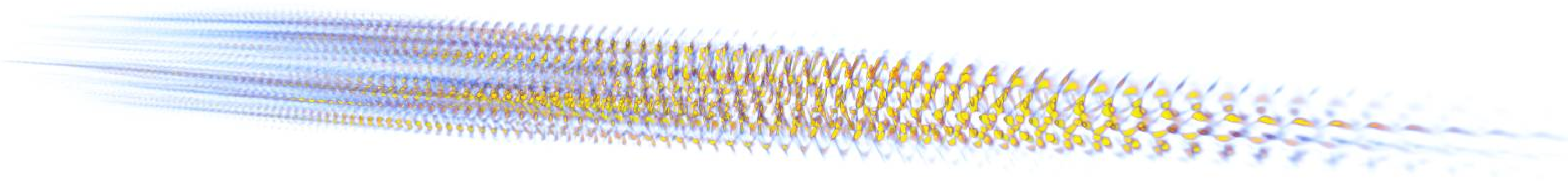

Wakefield-Driven Filamentation

Beam propagates into plasma prone to numerous instabilities

Beam property	Mitigates
Relativistic	Longitudinal motion
Quasineutral	Self-modulation
Dilute	Current filamentation

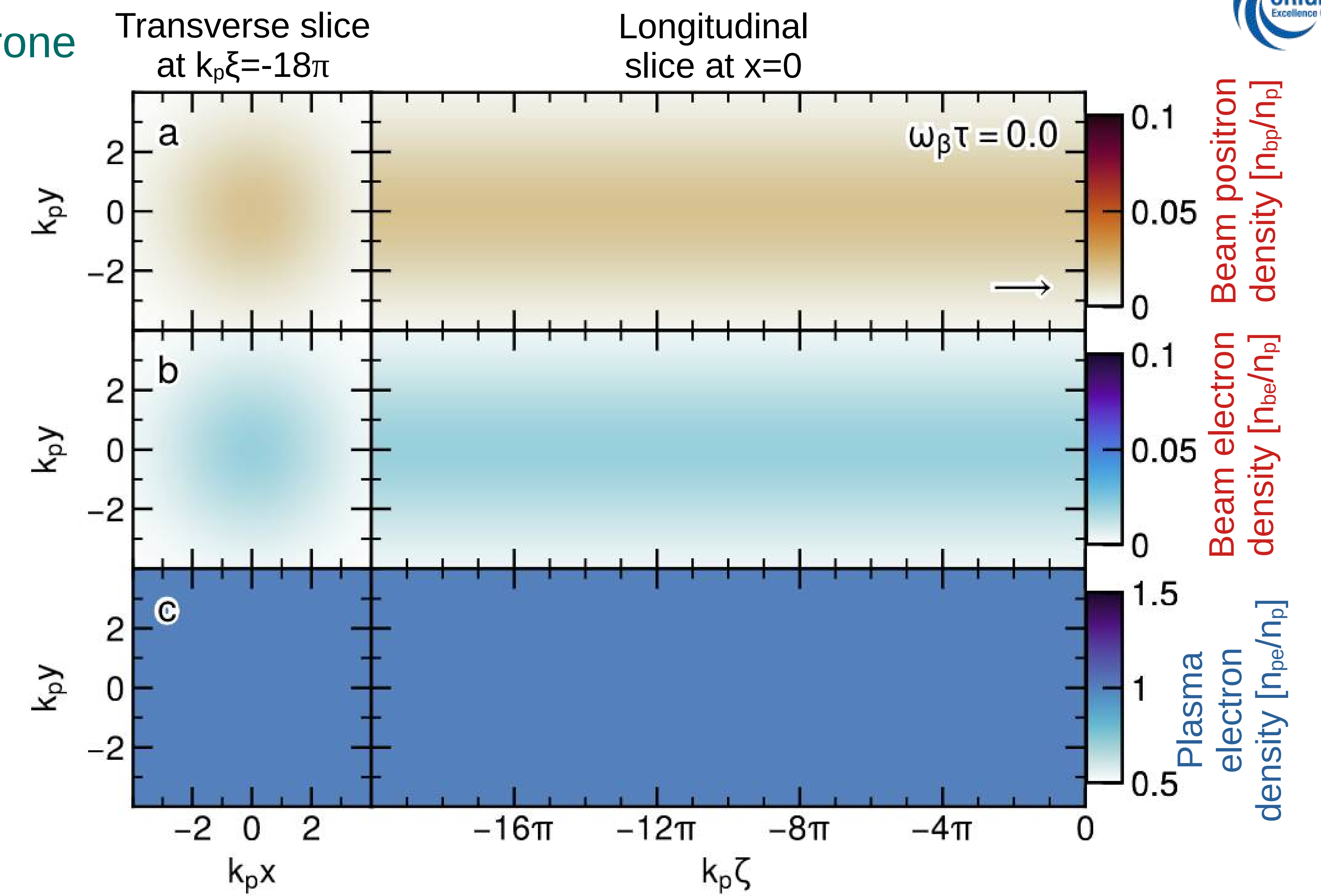

Wakefield-Driven Filamentation

Beam propagates into plasma prone to numerous instabilities

Beam property	Mitigates
Relativistic	Longitudinal motion
Quasineutral	Self-modulation
Dilute	Current filamentation

Beam and plasma filament with a longitudinal modulation from the plasma wakefield.

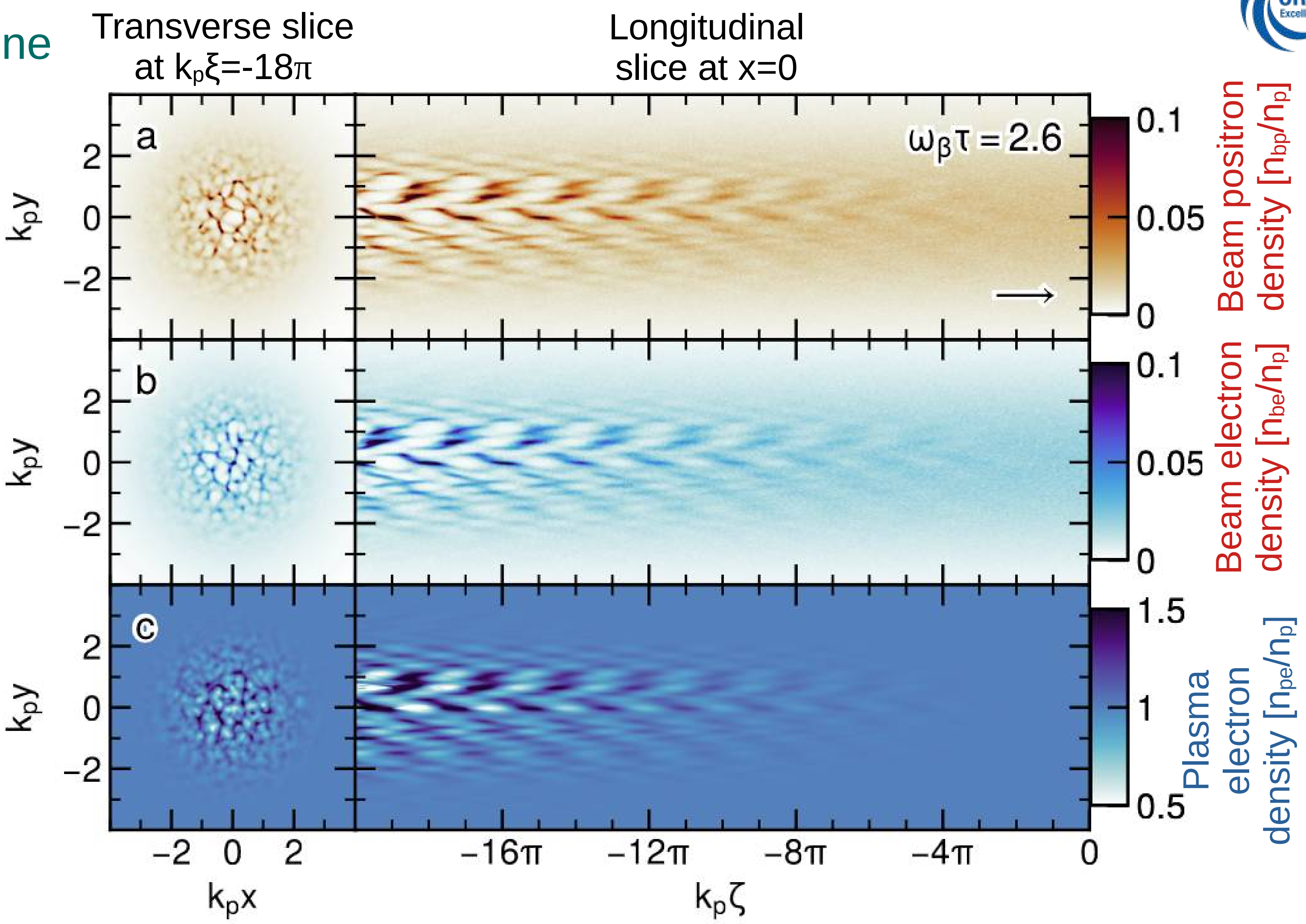

Wakefield-Driven Filamentation

Analytic model for the plasma response to a beam.

Wakefield-Driven Filamentation

Analytic model for the plasma response to a beam. →**Ansatz**: Wave-equation of EM-field

$$(\partial_\zeta^2 + k_e^2)(\nabla_\perp^2 - k_p^2)E_z = \partial_\zeta \rho_b/\varepsilon_0$$

$$(\partial_\zeta^2 + k_e^2)(\nabla_\perp^2 - k_p^2)\mathbf{W}_\perp = \nabla_\perp \rho_b/\varepsilon_0$$

$$k_e = ck_p/u_b$$

- Dilute beam → Negligible bulk plasma current
- Relativistic beam → Quasistatic approximation

Wakefield-Driven Filamentation

Analytic model for the plasma response to a beam. → **Ansatz**: Wave-equation of EM-field

$$(\partial_\zeta^2 + k_e^2)(\nabla_\perp^2 - k_p^2)E_z = \partial_\zeta \rho_b/\varepsilon_0$$

$$(\partial_\zeta^2 + k_e^2)(\nabla_\perp^2 - k_p^2)\mathbf{W}_\perp = \nabla_\perp \rho_b/\varepsilon_0$$

$$k_e = ck_p/u_b$$

- Dilute beam → Negligible bulk plasma current
- Relativistic beam → Quasistatic approximation

Initial beam charge perturbation (seed)

$$\rho_{b0} = q_b \delta n_{b0} f(\zeta) g(x,y)$$

$$g(x,y) = \tilde{g}(x,y)\cos(k_x x + \varphi_x)\cos(k_y y + \varphi_y)$$

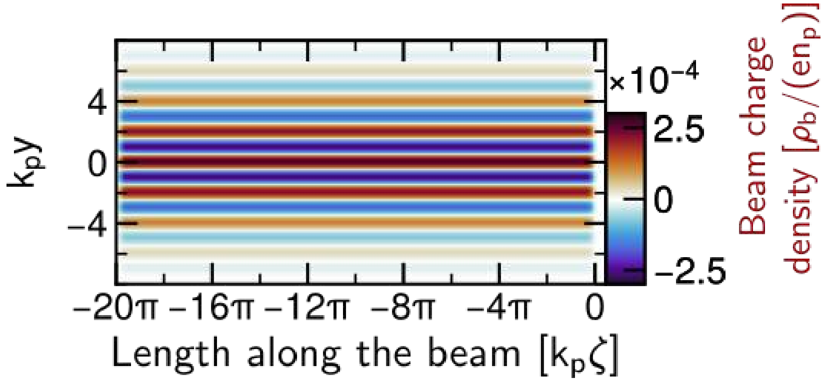

Wakefield-Driven Filamentation

Analytic model for the plasma response to a beam. → **Ansatz**: Wave-equation of EM-field

$$(\partial_\zeta^2 + k_e^2)(\nabla_\perp^2 - k_p^2)E_z = \partial_\zeta \rho_b/\varepsilon_0$$
$$(\partial_\zeta^2 + k_e^2)(\nabla_\perp^2 - k_p^2)\mathbf{W}_\perp = \nabla_\perp \rho_b/\varepsilon_0$$
$$k_e = ck_p/u_b$$

- Dilute beam → Negligible bulk plasma current
- Relativistic beam → Quasistatic approximation

Initial beam charge perturbation (seed)

$$\rho_{b0} = q_b \delta n_{b0} f(\zeta) g(x,y)$$
$$g(x,y) = \tilde{g}(x,y)\cos(k_x x + \varphi_x)\cos(k_y y + \varphi_y)$$

Excited plasma wakefield

$$E_z = \frac{q_b \delta n_b}{\varepsilon_0}\frac{k_e^2 g(x,y)}{k_e^2 + k_r^2}\int_\zeta^0 \mathrm{d}\zeta' f(\zeta')\cos k_e(\zeta - \zeta')$$

$$\mathbf{W}_\perp = \frac{q_b \delta n_b}{\varepsilon_0}\frac{k_e \nabla_\perp g(x,y)}{k_e^2 + k_r^2}\int_\zeta^0 \mathrm{d}\zeta' f(\zeta')\sin k_e(\zeta - \zeta')$$

$$k_r = \sqrt{k_x^2 + k_y^2}$$

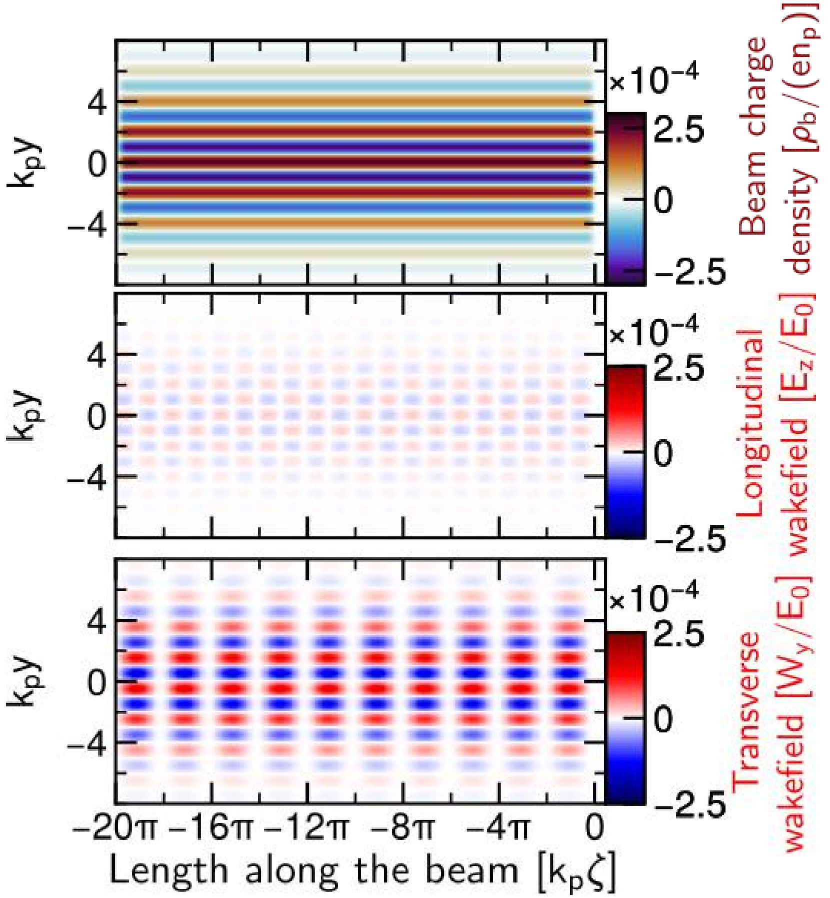

Filamentation of Cold Beams

The wakefield acts back on the beam.

- The perturbation and electric field evolves along the length of the beam and plasma.
- Weak local magnetic field from the beam current

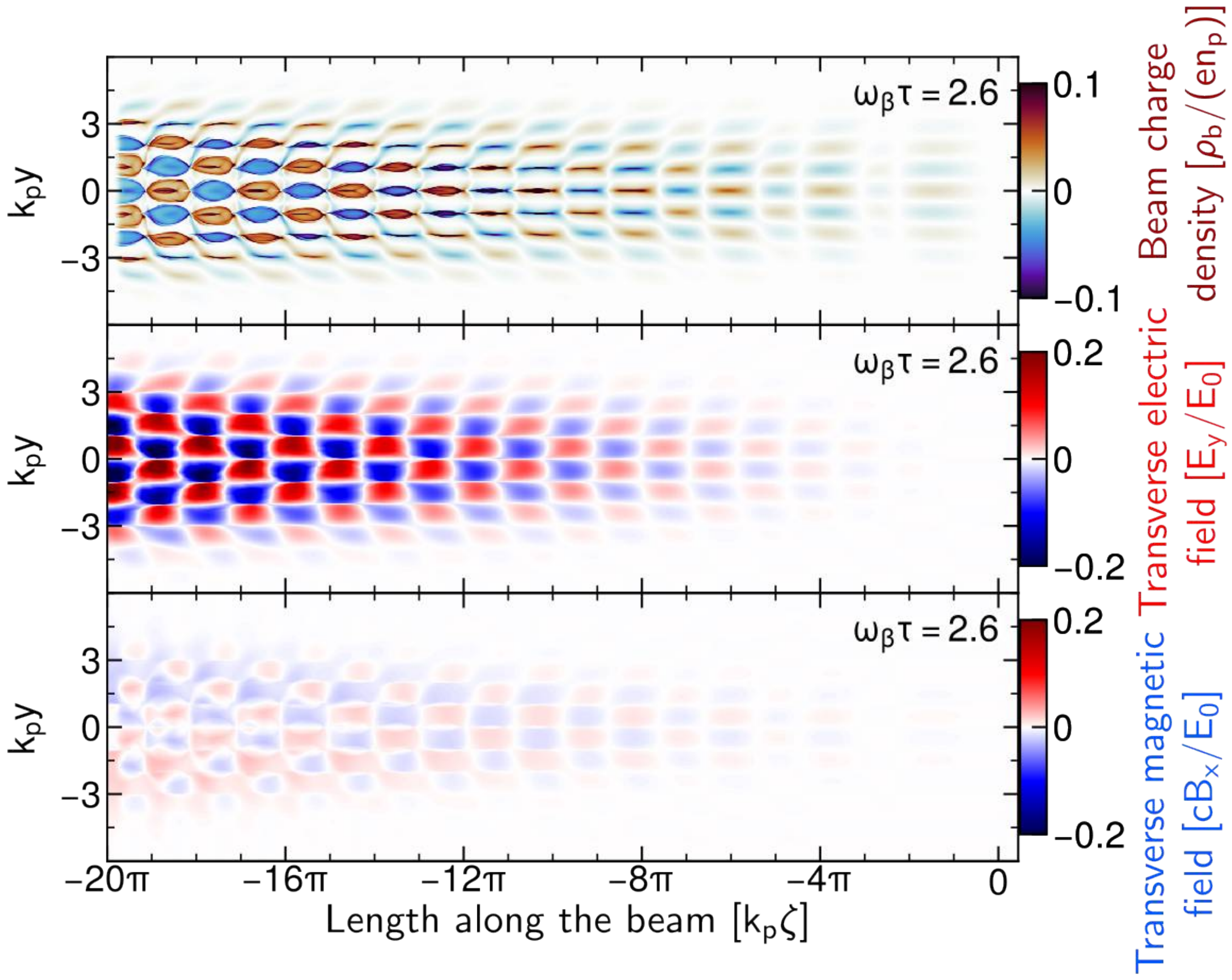

Filamentation of Cold Beams

The wakefield acts back on the beam.

- The perturbation and electric field evolves along the length of the beam and plasma.
- Weak local magnetic field from the beam current

Ansatz: Cold fluid equation

Beam particles are	accelerated/ decelerated	focussed/ defocussed

$$\partial_\tau^2 \delta n_b = \frac{2\omega_\beta^2}{q_b/\varepsilon_0}\left(\boxed{\frac{\partial_z E_z}{\gamma_b^2}} + \boxed{\nabla_\perp \cdot \mathbf{W}_\perp}\right)$$

$$\omega_\beta = \sqrt{q_b n_b^2/(2\gamma_b \varepsilon_0 m_b)}$$

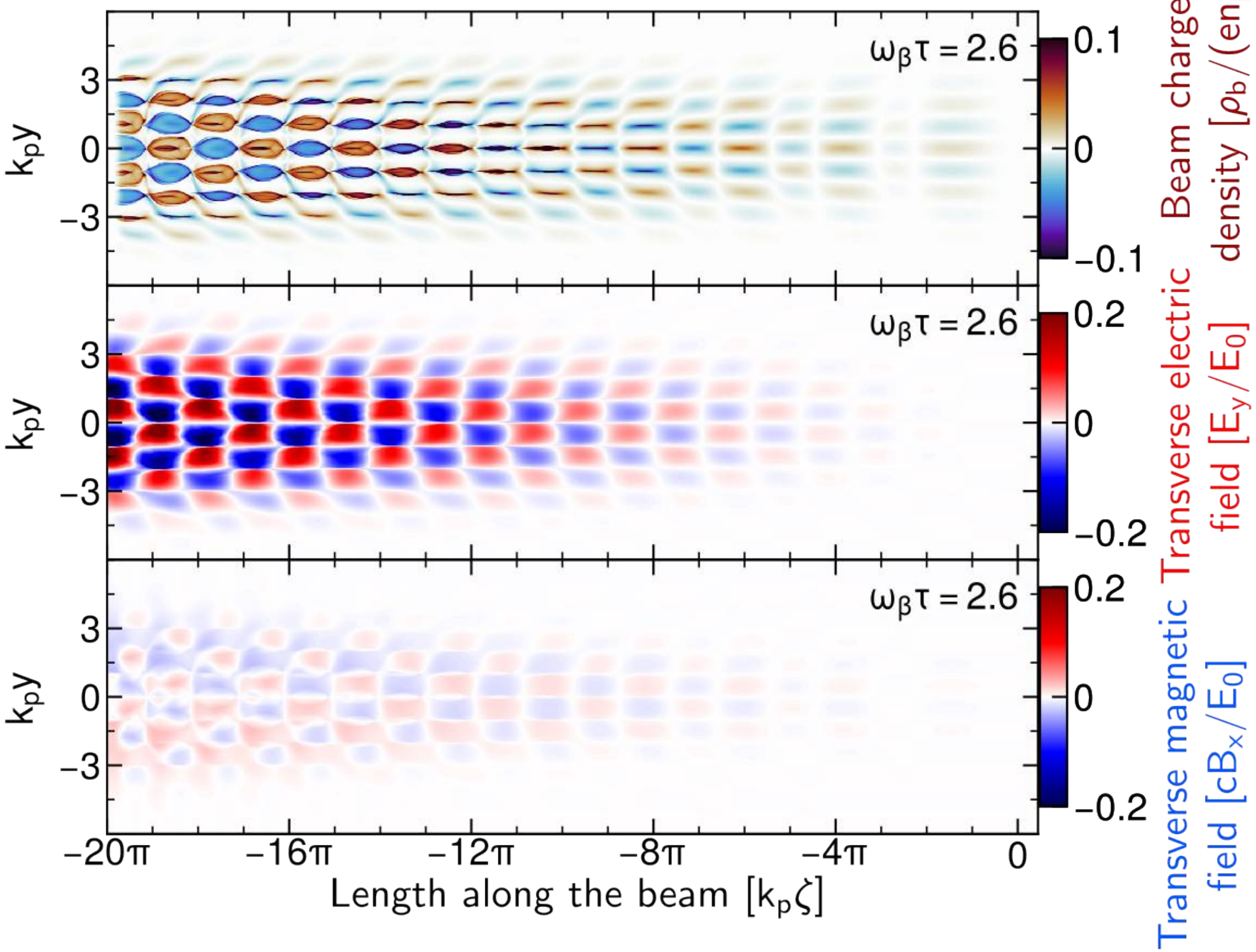

Filamentation of Cold Beams

The wakefield acts back on the beam.

- The perturbation and electric field evolves along the length of the beam and plasma.
- Weak local magnetic field from the beam current

Ansatz: Cold fluid equation

Beam particles are accelerated/ decelerated focussed/ defocussed

$$\partial_\tau^2 \delta n_b = \frac{2\omega_\beta^2}{q_b/\varepsilon_0}\left(\boxed{\frac{\partial_z E_z}{\gamma_b^2}} + \boxed{\nabla_\perp \cdot \mathbf{W}_\perp}\right)$$

$$\omega_\beta = \sqrt{q_b n_b^2/(2\gamma_b \varepsilon_0 m_b)}$$

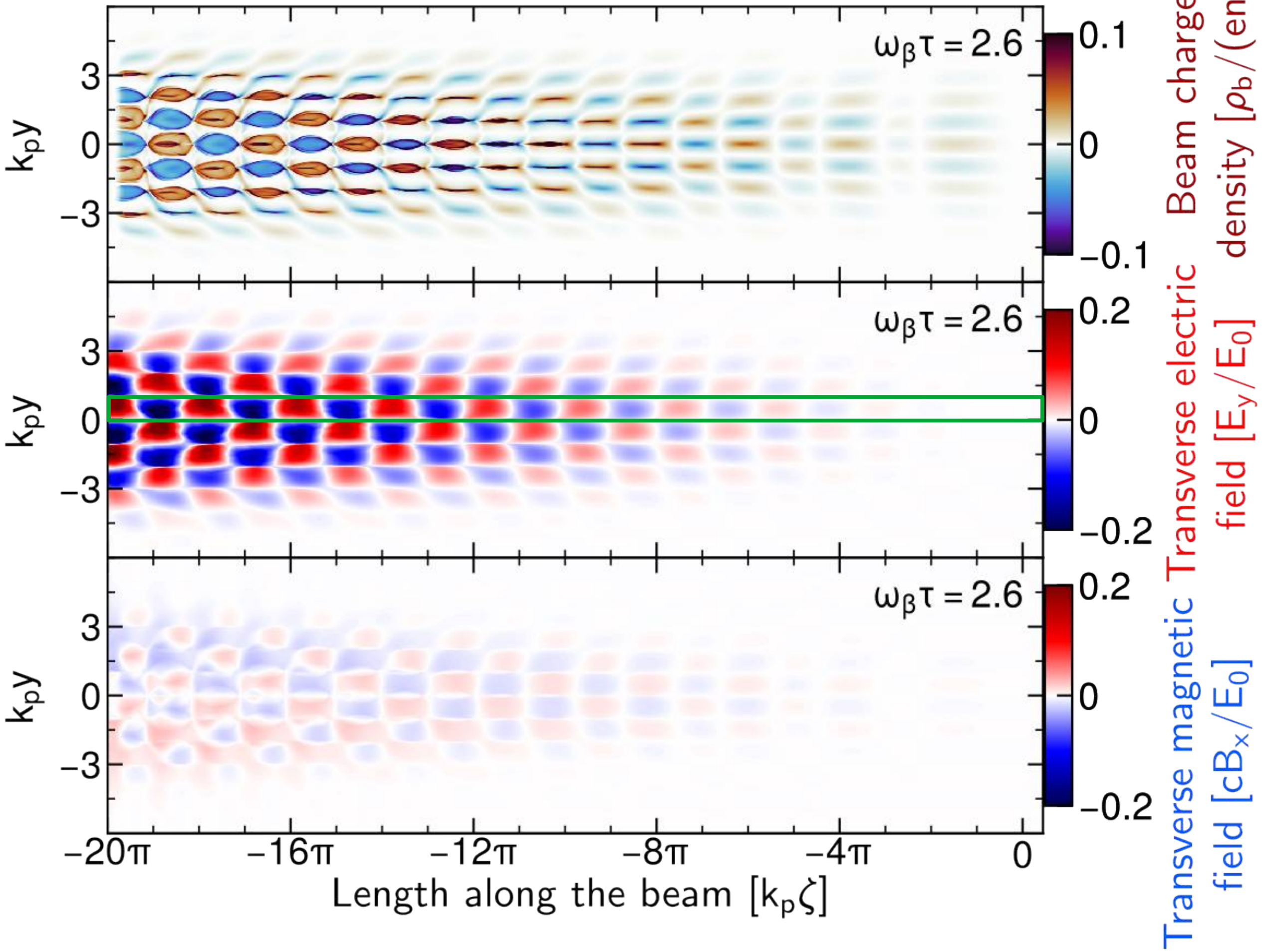

Filamentation of Cold Beams

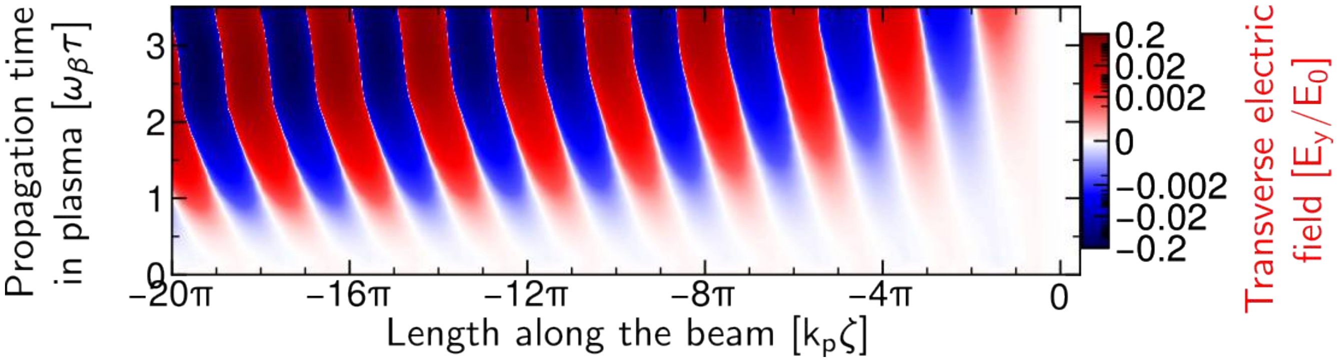

Filamentation of Cold Beams

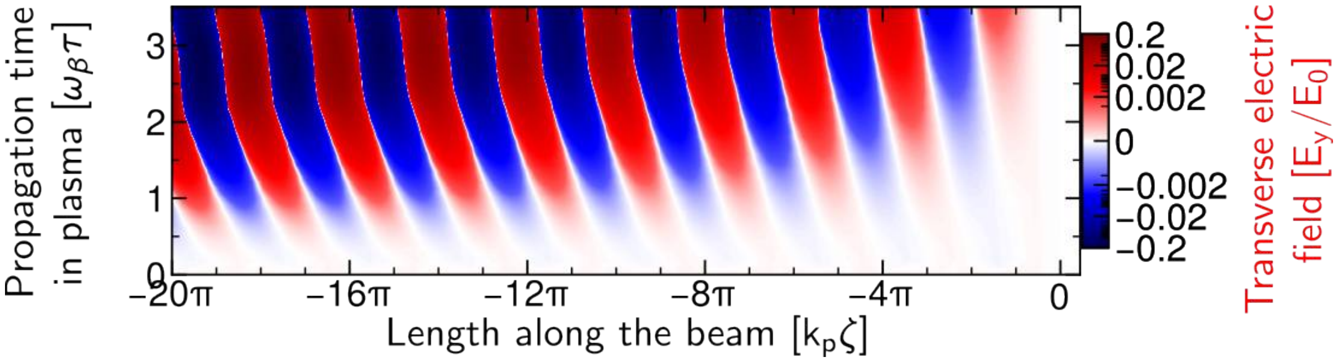

Analytic expression for the **growth**

$$\boxed{\begin{aligned}\Gamma_{\mathrm{ts}} &= \frac{\delta n_{b,\mathrm{ts}}}{\delta n_{b0}} = \left|\sum_{l=0}^{\infty} \frac{(i\eta_u)^l}{l!(2l)!}\right| \\ &\approx \frac{1}{\sqrt{4\pi}} \frac{\exp N_\infty}{\sqrt{N_\infty}}\end{aligned}}$$

$$\eta_u = \frac{(c^2 - u_b^2)k_p^2 + u_b^2 k_r^2}{c^2 k_p^2 + u_b^2 k_r^2}$$ spectral factor

$$\times\, \tilde{g}(x,y)$$ local stream density

$$\times\, k_e \left| \int_\zeta^0 \tilde{f}(\zeta')\mathrm{d}\zeta' \right| \omega_\beta^2 \tau^2$$ spatiotemporal growth

$$N_\infty = \frac{3^{3/2}}{2^{5/3}} \eta_u^{1/3}$$ Number of e-foldings

Filamentation of Cold Beams

Analytic expression for the **growth**

$$\boxed{\begin{aligned}\Gamma_{\mathrm{ts}} = \frac{\delta n_{b,\mathrm{ts}}}{\delta n_{b0}} &= \left| \sum_{l=0}^{\infty} \frac{(i\eta_u)^l}{l!(2l)!} \right| \\ &\approx \frac{1}{\sqrt{4\pi}} \frac{\exp N_\infty}{\sqrt{N_\infty}}\end{aligned}}$$

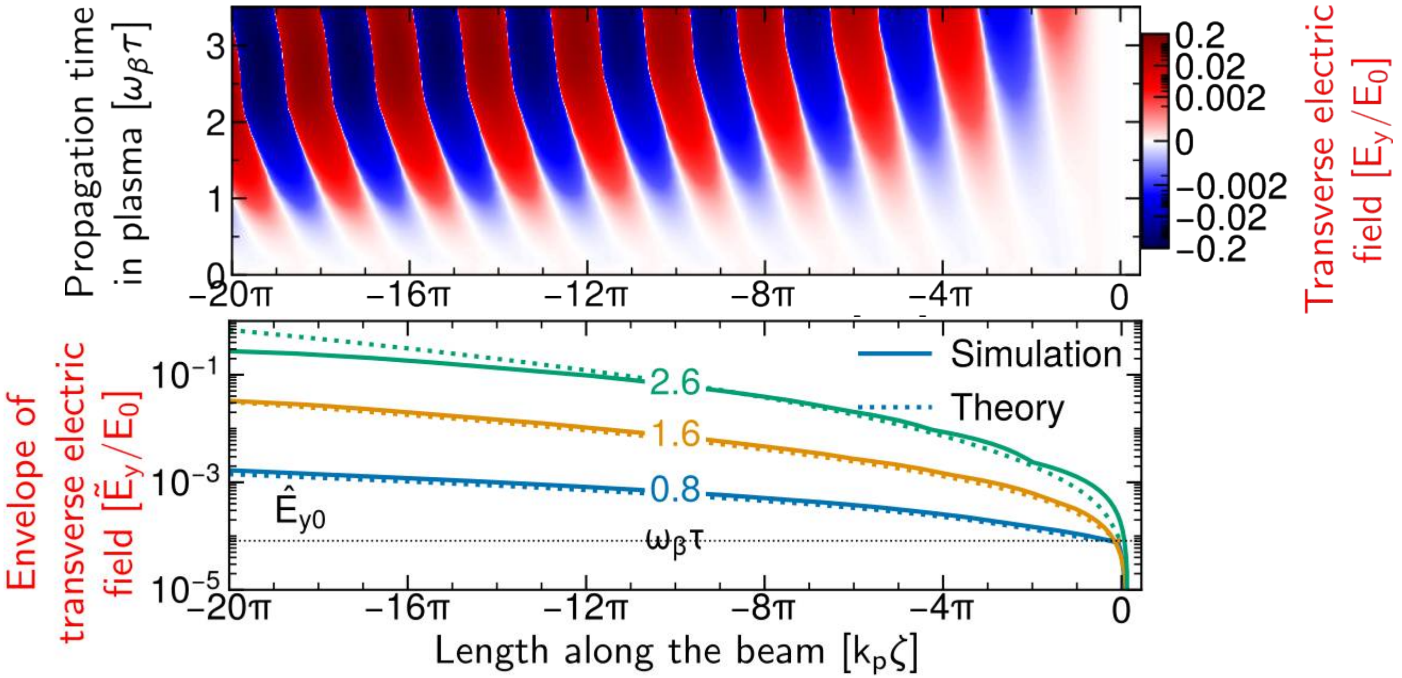

$$\eta_u = \frac{(c^2 - u_b^2)k_p^2 + u_b^2 k_r^2}{c^2 k_p^2 + u_b^2 k_r^2}$$ spectral factor

$$\times\, \tilde{g}(x,y)$$ local stream density

$$\times\, k_e \left| \int_\zeta^0 \tilde{f}(\zeta')\mathrm{d}\zeta' \right| \omega_\beta^2 \tau^2$$ spatiotemporal growth

$$N_\infty = \frac{3^{3/2}}{2^{5/3}} \eta_u^{1/3}$$ Number of e-foldings

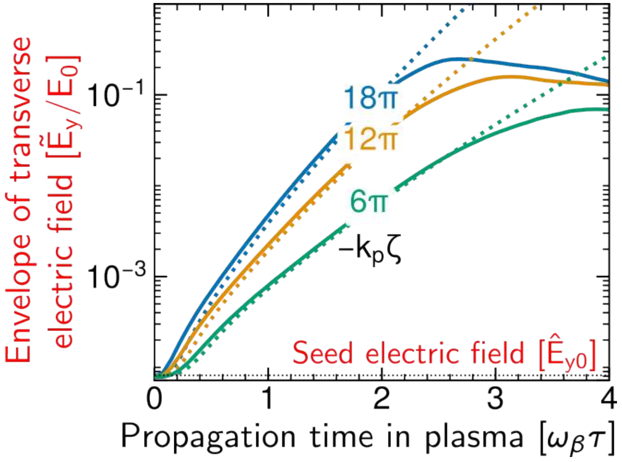

Filamentation of Cold Beams

Phase velocity

$$u_\psi = u_b \left[1 - \frac{2}{3^{3/2}} \frac{N_\infty}{\omega_p \tau} \right]$$

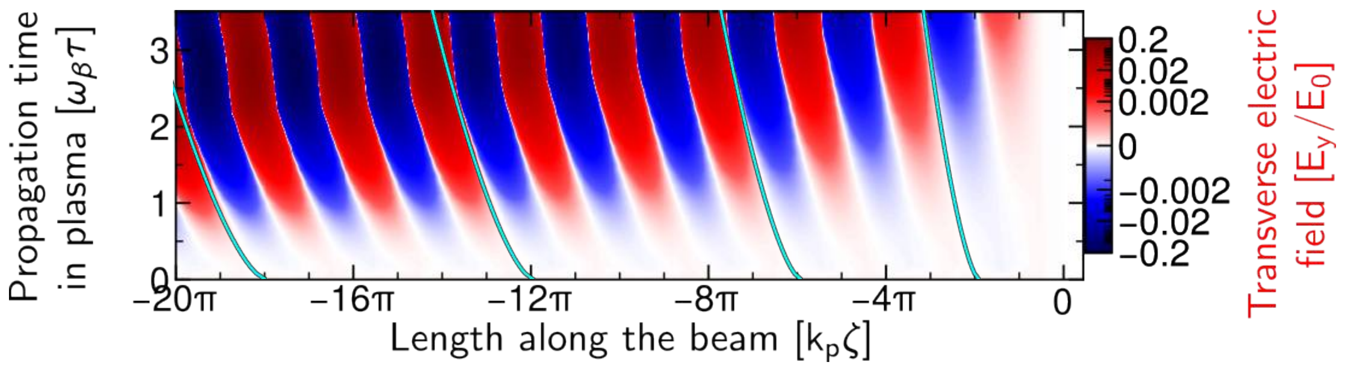

Analytical model tracks growth and phase of the wakefield

- Expression for the beam perturbation agrees with Claveria *et al.*, PRR, 2022 for the plasma perturbation
- BUT filament spacing limited by the grid resolution
- **What determines the filament spacing physically?**

Filamentation of Warm Beams

Phase and transverse modulation deviates from the case of the cold beam

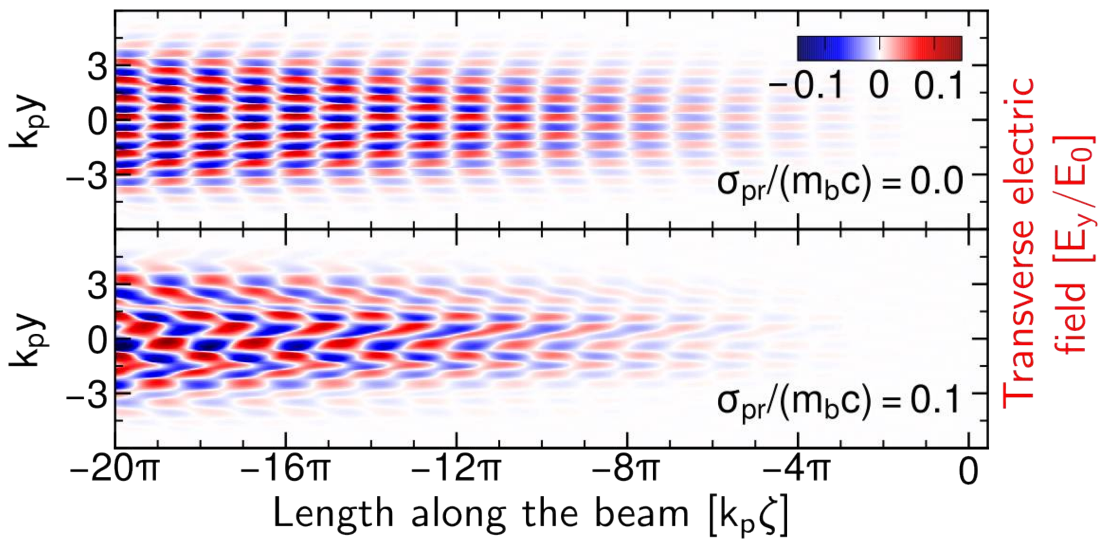

Filamentation of Warm Beams

Phase and transverse modulation deviates from the case of the cold beam

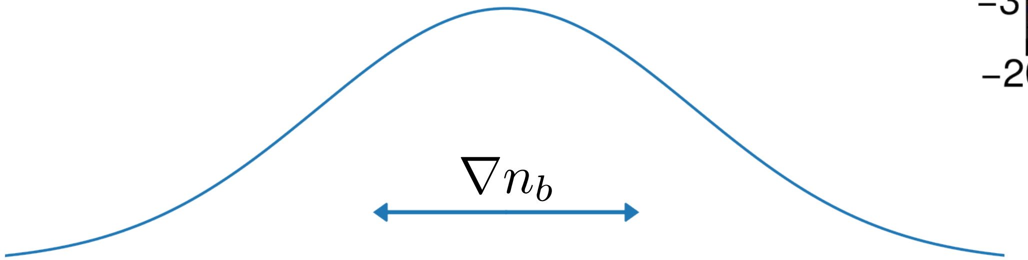

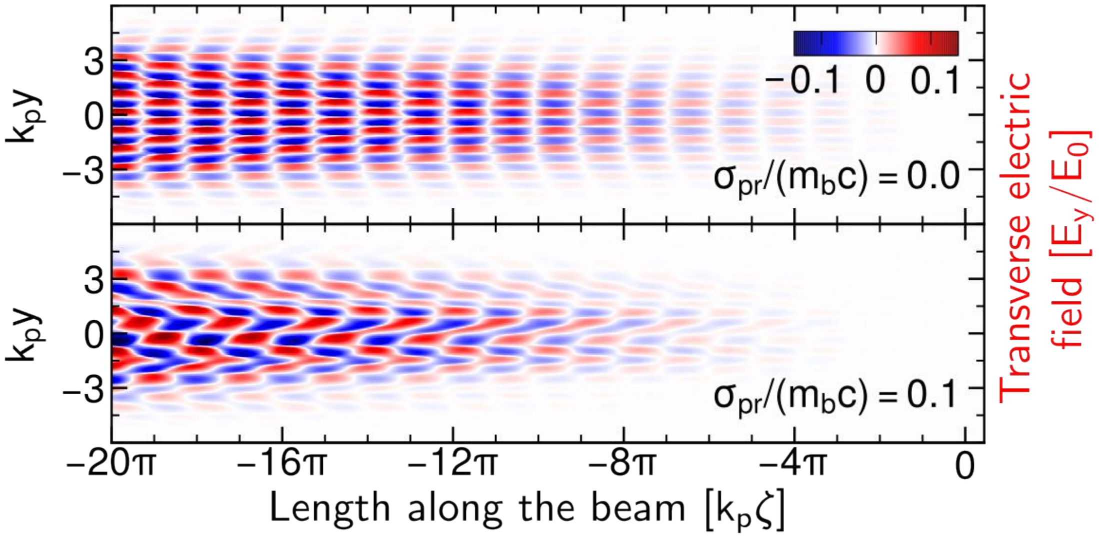

Filamentation of Warm Beams

Phase and transverse modulation deviates from the case of the cold beam

- Diffusion causes fine-scale perturbations to spread out

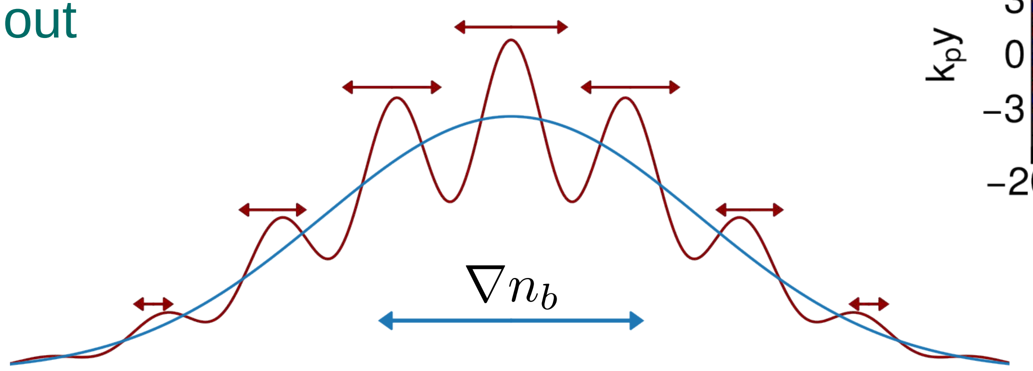

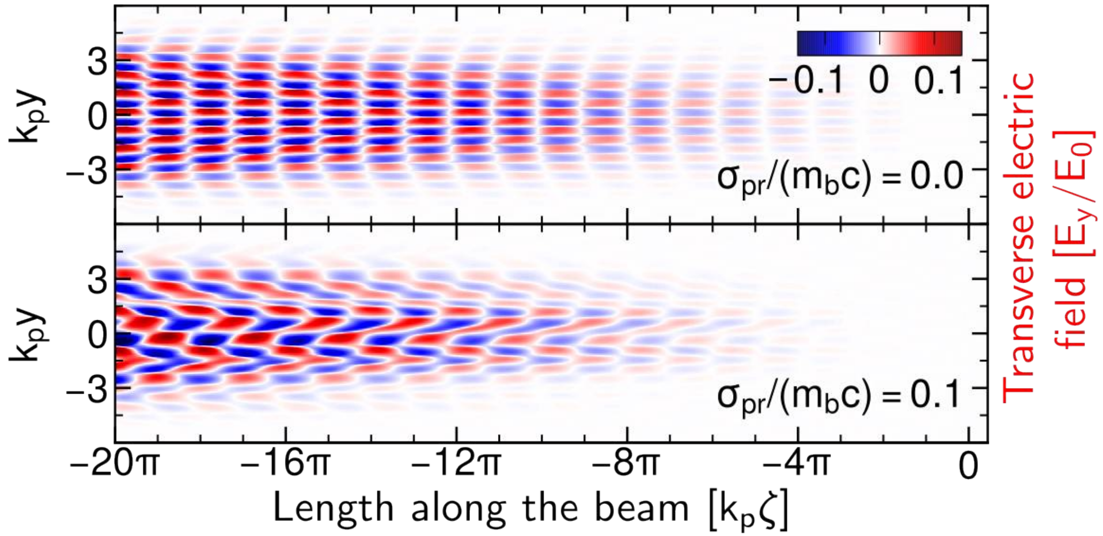

Filamentation of Warm Beams

Phase and transverse modulation deviates from the case of the cold beam

- Diffusion causes fine-scale perturbations to spread out

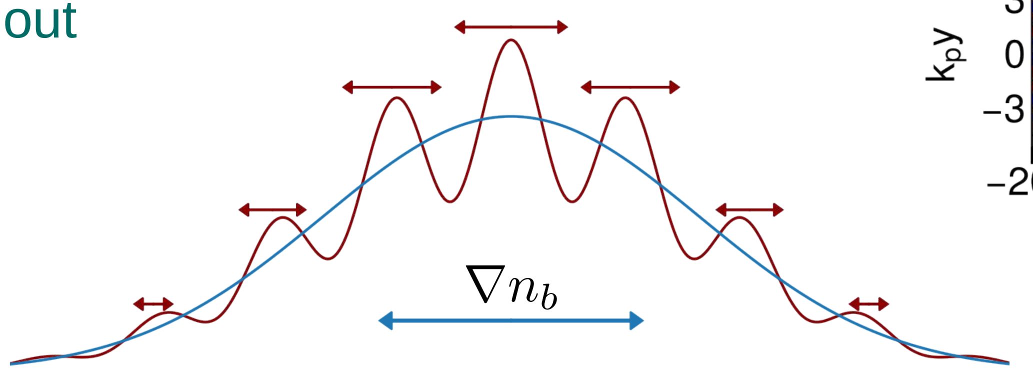

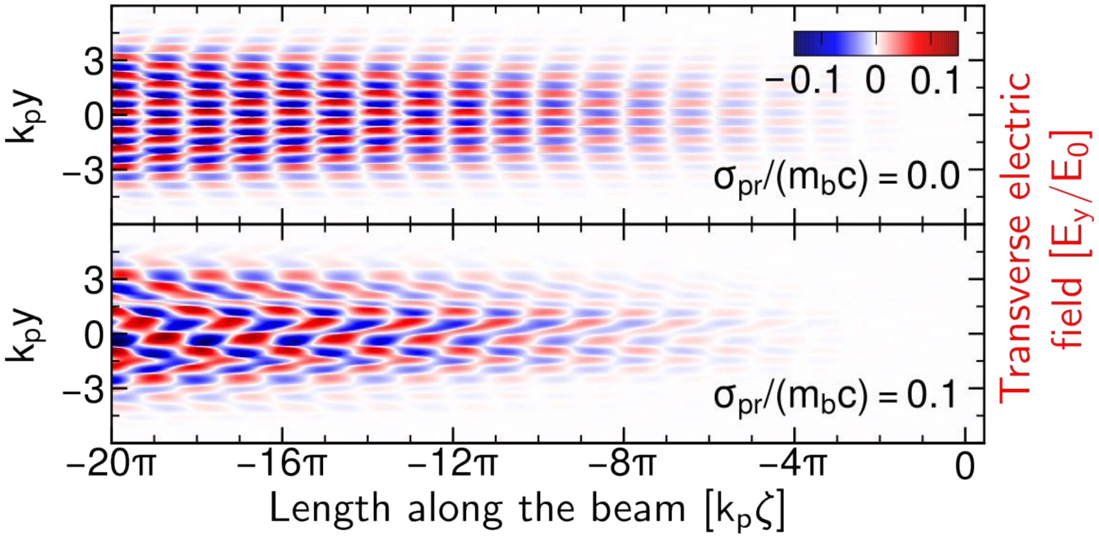

Ansatz: Extend fluid equation by thermal pressure term

$$\left(\partial_\tau^2 + \boxed{\frac{2}{3}\frac{\sigma_{pr}^2}{m_b^2\gamma_b^2}\nabla_\perp^2}\right)\delta n_b = \frac{2\omega_\beta^2}{q_b/\varepsilon_0}\left(\frac{\partial_z E_z}{\gamma_b^2} + \nabla_\perp \cdot \mathbf{W}_\perp\right)$$

Filamentation of Warm Beams

Phase and transverse modulation deviates from the case of the cold beam

- Diffusion causes fine-scale perturbations to spread out

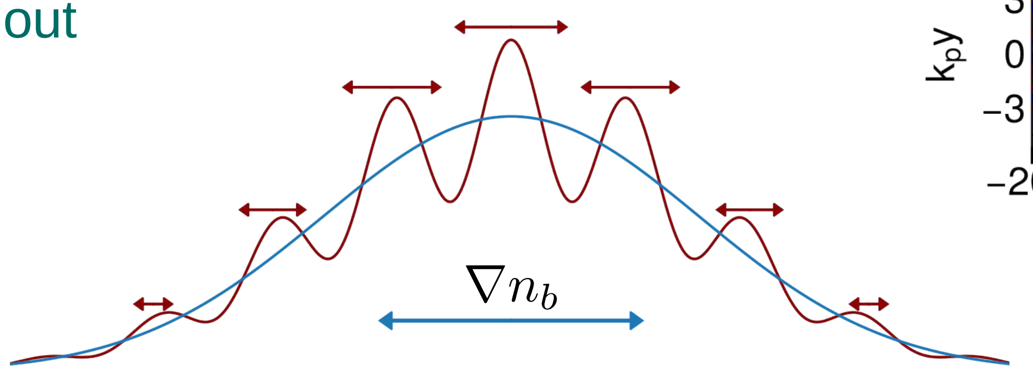

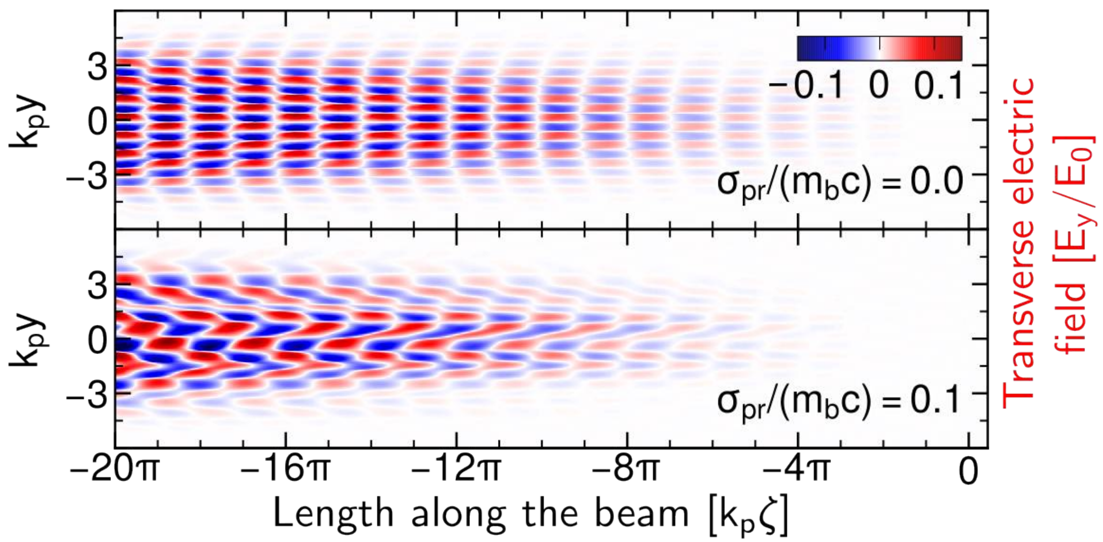

Ansatz: Extend fluid equation by thermal pressure term

$$\left(\partial_\tau^2 + \boxed{\frac{2}{3}\frac{\sigma_{pr}^2}{m_b^2\gamma_b^2}\nabla_\perp^2}\right)\delta n_b = \frac{2\omega_\beta^2}{q_b/\varepsilon_0}\left(\frac{\partial_z E_z}{\gamma_b^2} + \nabla_\perp \cdot \mathbf{W}_\perp\right)$$

Growth rate for transverse two-stream reduces

$$\boxed{\Gamma_{\text{tot}} = \frac{\delta n_b}{\delta n_{b0}} = \Gamma_{\text{ts}} \exp\left(-\nu_d \tau\right), \quad \nu_d = \sqrt{\frac{2}{3}}\frac{\sigma_{pr} k_r}{\gamma_b m_b}}$$

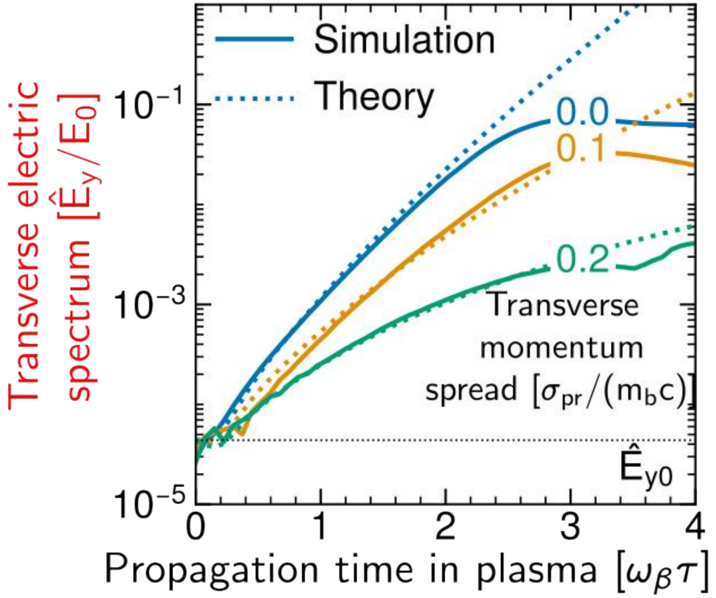

Filamentation of Warm Beams

Full spectrum of the non-seeded warm beam

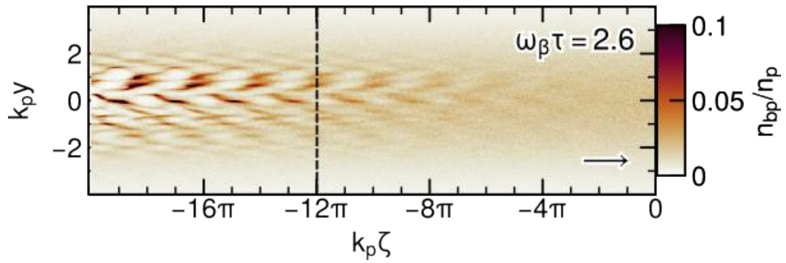

Filamentation of Warm Beams

Full spectrum of the non-seeded warm beam

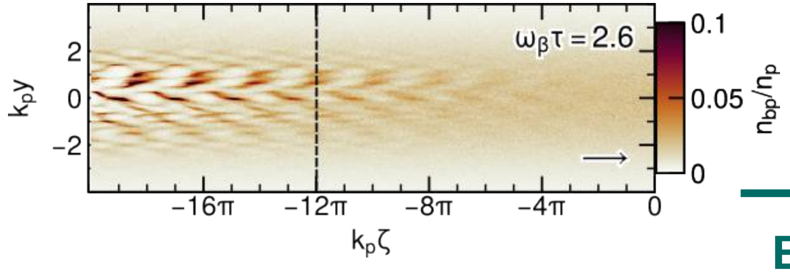

$E_\perp$ at $k_p\xi$=-12π

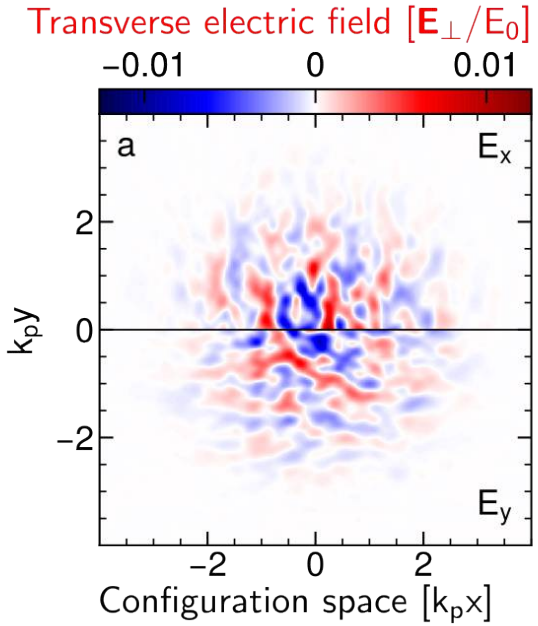

Filamentation of Warm Beams

Full spectrum of the non-seeded warm beam

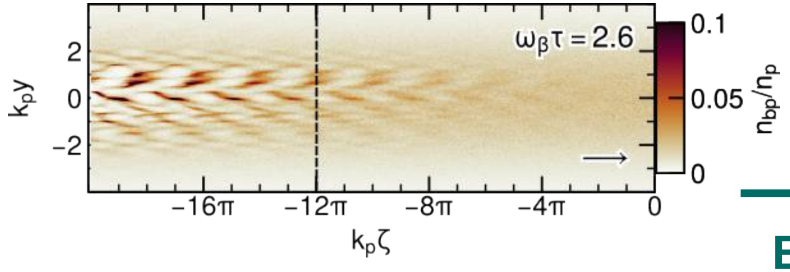

$E_\perp$ at
$k_p\xi$=-12π

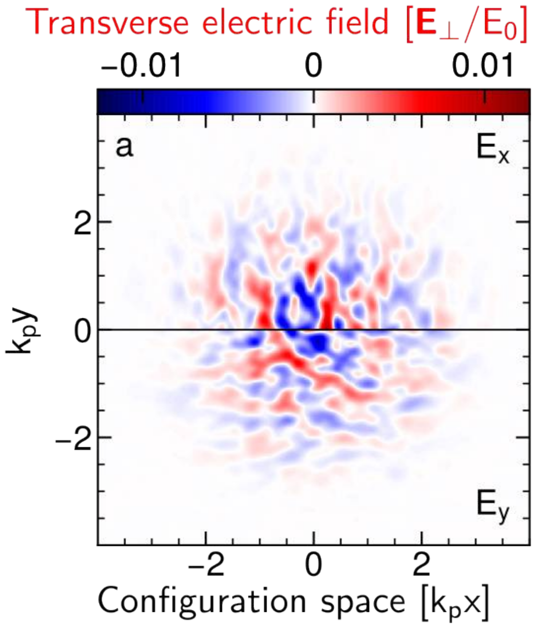

Fourier transform

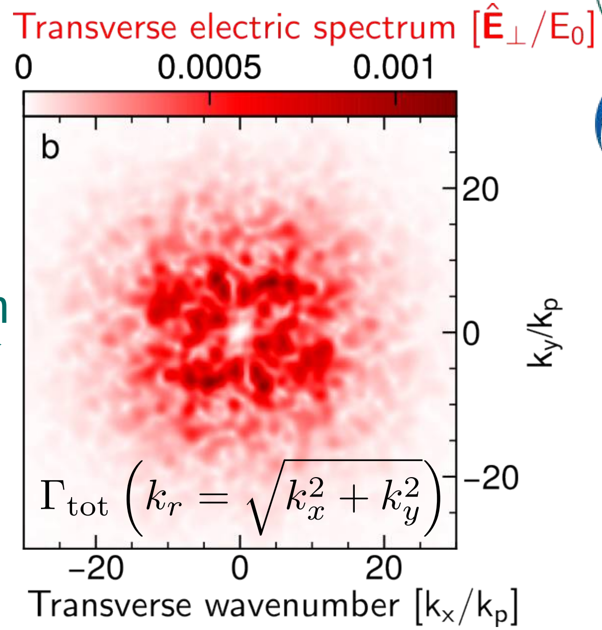

Filamentation of Warm Beams

Full spectrum of the non-seeded warm beam

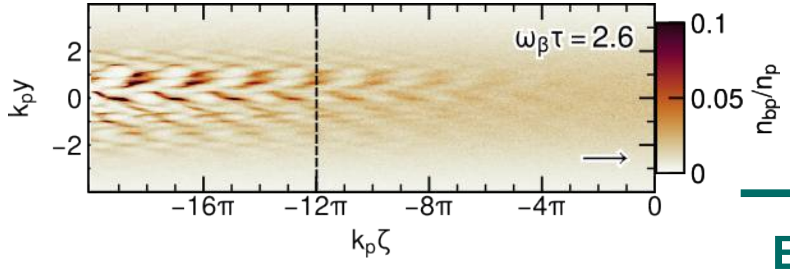

$\mathbf{E}_\perp$ at $k_p\xi=-12\pi$

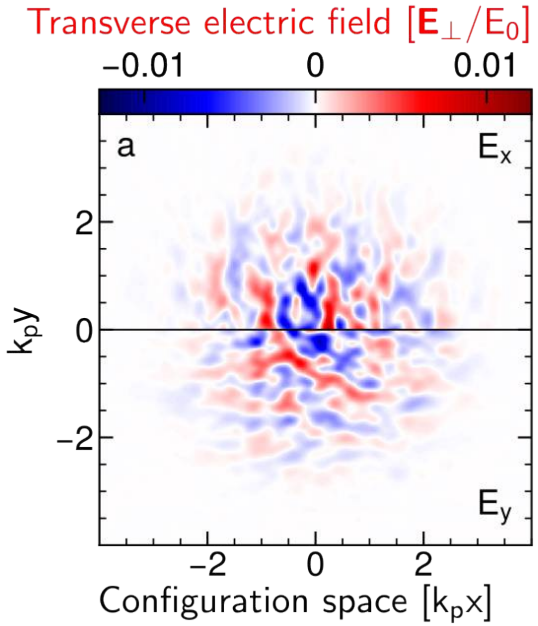

Fourier transform

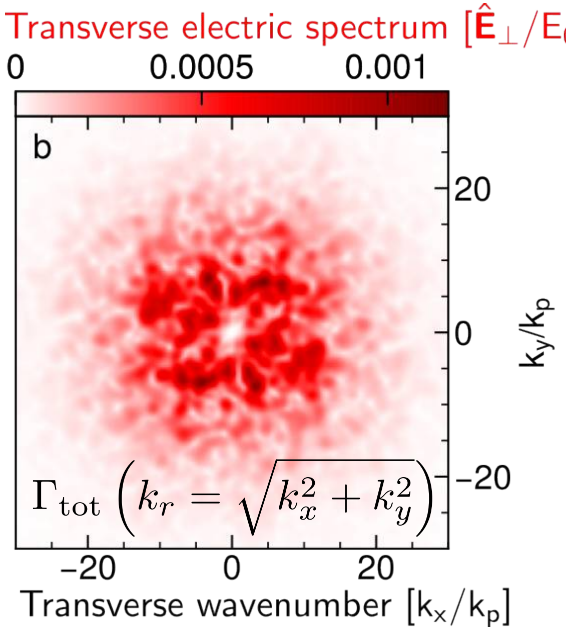

Average over all orientations

Fine scale filaments grow faster for $k_r<k_{Emax}$, higher wavenumbers are damped by diffusion.

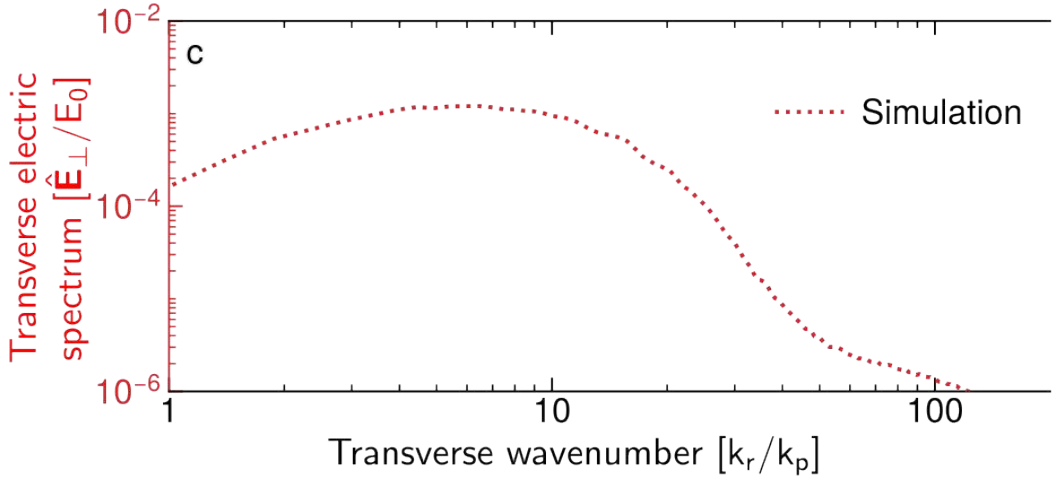

Filamentation of Warm Beams

Full spectrum of the non-seeded warm beam

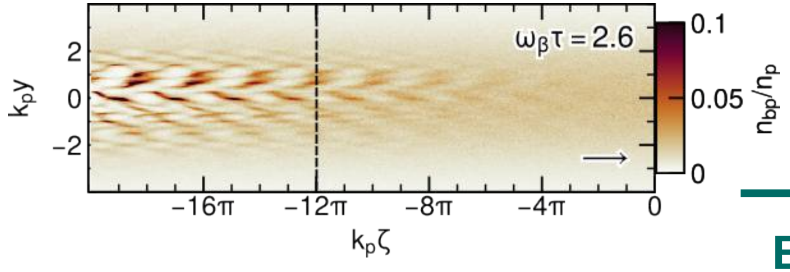

$E_\perp$ at $k_p\xi$=-12π

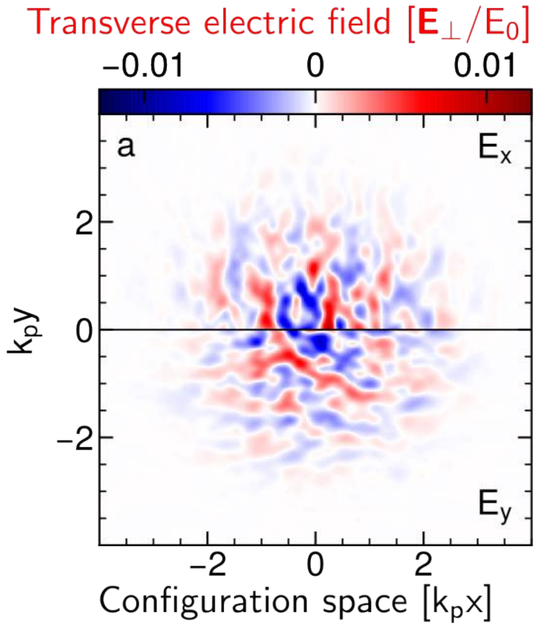

Fourier transform

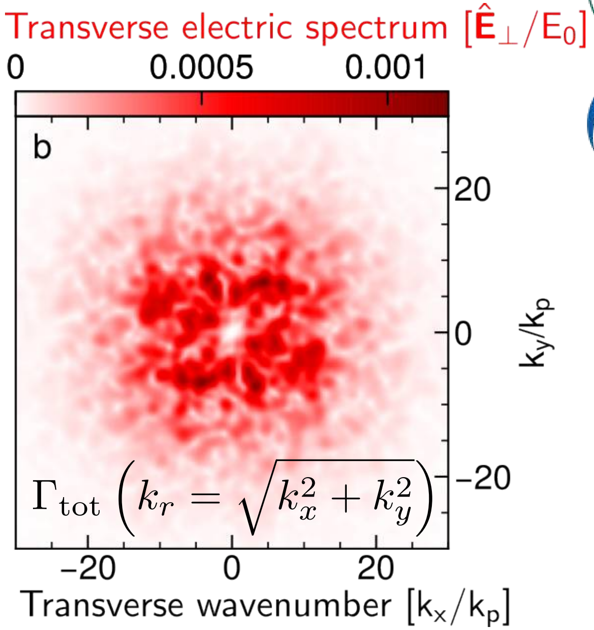

Average over all orientations

Fine scale filaments grow faster for k_r<k_{Emax}, higher wavenumbers are damped by diffusion.

$$|\hat{E}_\perp| = |\hat{E}_{\perp 0}(k_r)|\Gamma_{\text{tot}}(k_r)$$

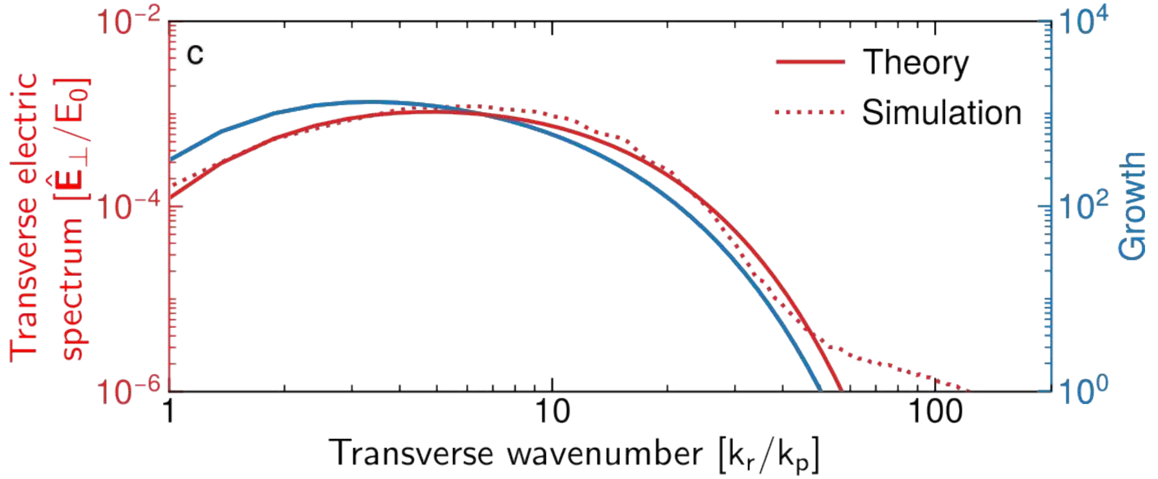

Filamentation of Warm Beams

Full spectrum of the non-seeded warm beam

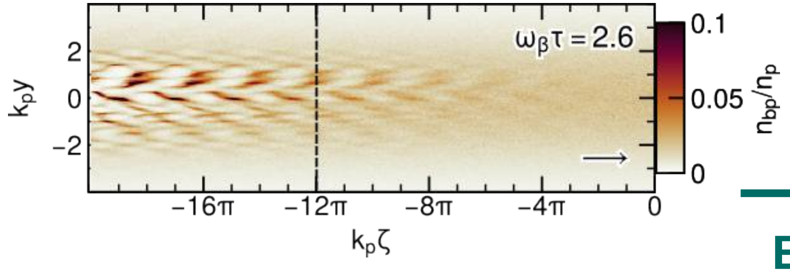

$E_\perp$ at
$k_p\xi$=-12π

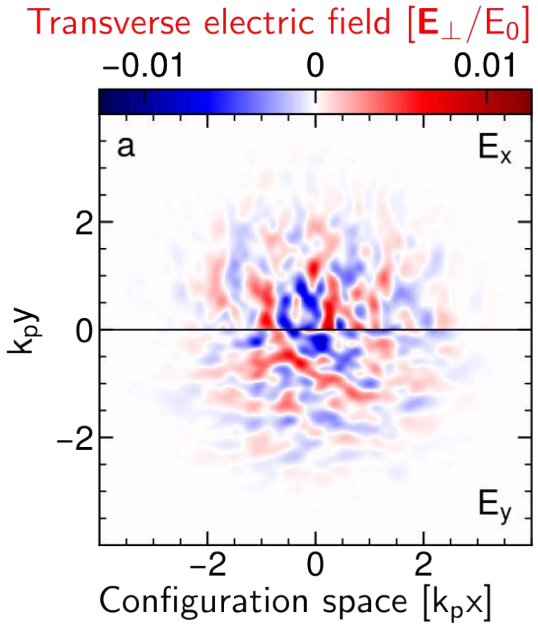

Fourier transform

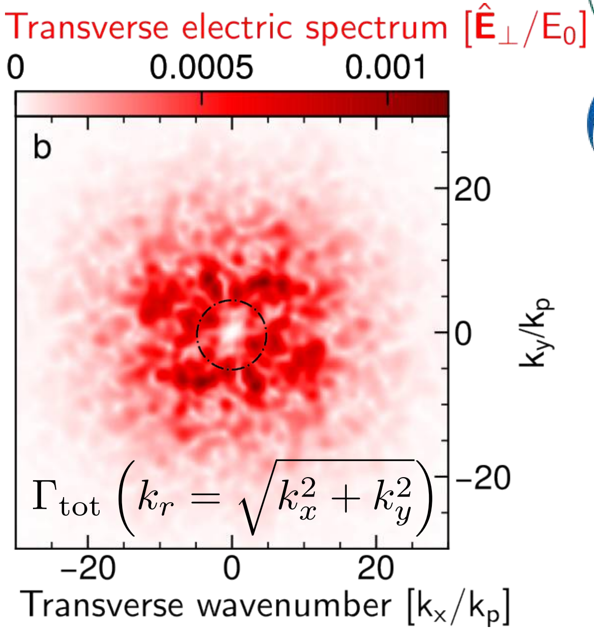

Average over all orientations

Fine scale filaments grow faster for $k_r < k_{Emax}$, higher wavenumbers are damped by diffusion.

$$|\hat{E}_\perp| = |\hat{E}_{\perp 0}(k_r)|\Gamma_{\text{tot}}(k_r)$$

$$N_\infty(k_{\text{cut}}) = \nu_d(k_{\text{cut}})\tau + \ln\sqrt{4\pi N_\infty(k_{\text{cut}})}$$

$$1 + 3k_{E_{\max}}^2 + 4N_\infty(k_{E_{\max}}) = 6(1 + k_{E_{\max}}^2)\nu_d(k_{E_{\max}})\tau$$

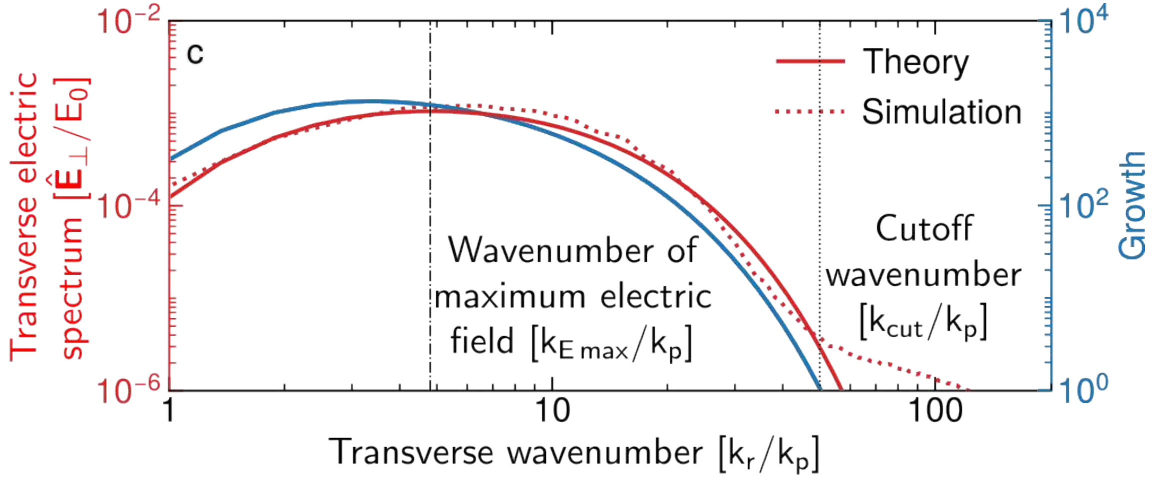

Spatiotemporal wavenumbers $k_{Emax}(\tau,\xi)$

Filamentation of Warm Beams

Full spectrum of a non-seeded warm beam

Excellent agreement of analytical model for wakefield-driven filamentation with two- and three-dimensional simulations.

- Efficiently modeled filaments in 2D are more tightly clustered
- Maximum growth decreases with temperature aligning with

$$2N_\infty(k_{\Gamma_{\max}}) = 3(1 + k_{\Gamma_{\max}}^2)\nu_d(k_{\Gamma_{\max}})\tau + 1$$

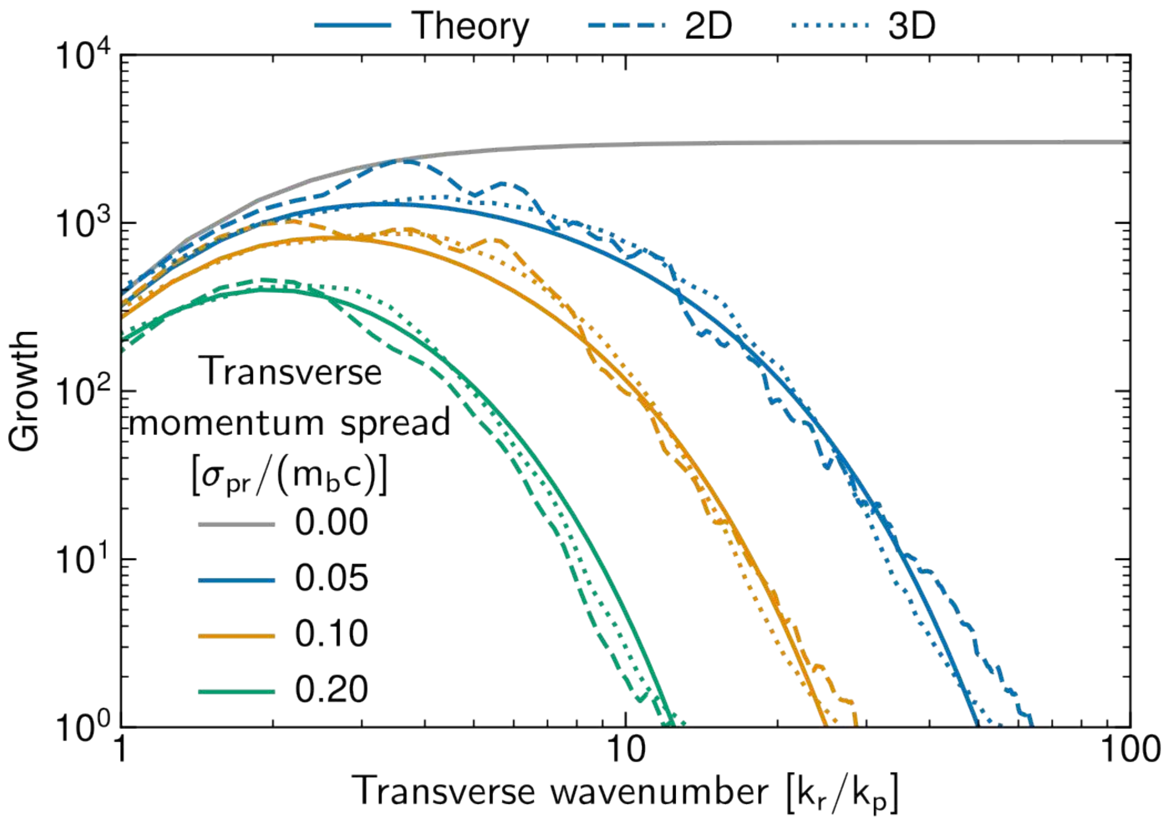

Experimental Observation of the Filamentation Instability

Expected filament spacing: $\lambda_f = 2\pi / k_{E\max}$

numerically evaluated from

$$1 + 3k_{E_{\max}}^2 + 4N_\infty(k_{E_{\max}}) = 6(1 + k_{E_{\max}}^2)\nu_d(k_{E_{\max}})\tau$$

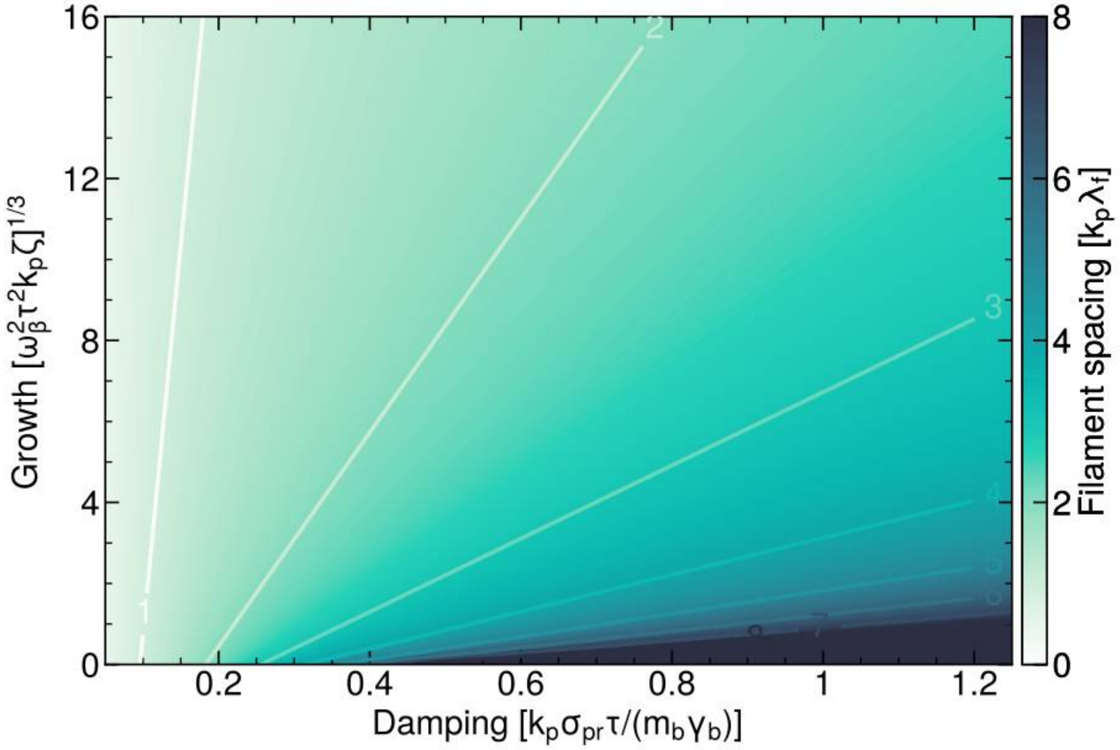

Experimental Observation of the Filamentation Instability

Expected filament spacing: $\lambda_f = 2\pi / k_{E\max}$
numerically evaluated from

$$1 + 3k_{E_{\max}}^2 + 4N_\infty(k_{E_{\max}}) = 6(1 + k_{E_{\max}}^2)\nu_d(k_{E_{\max}})\tau$$

Increase beam charge
➤ Filament spacing decreases

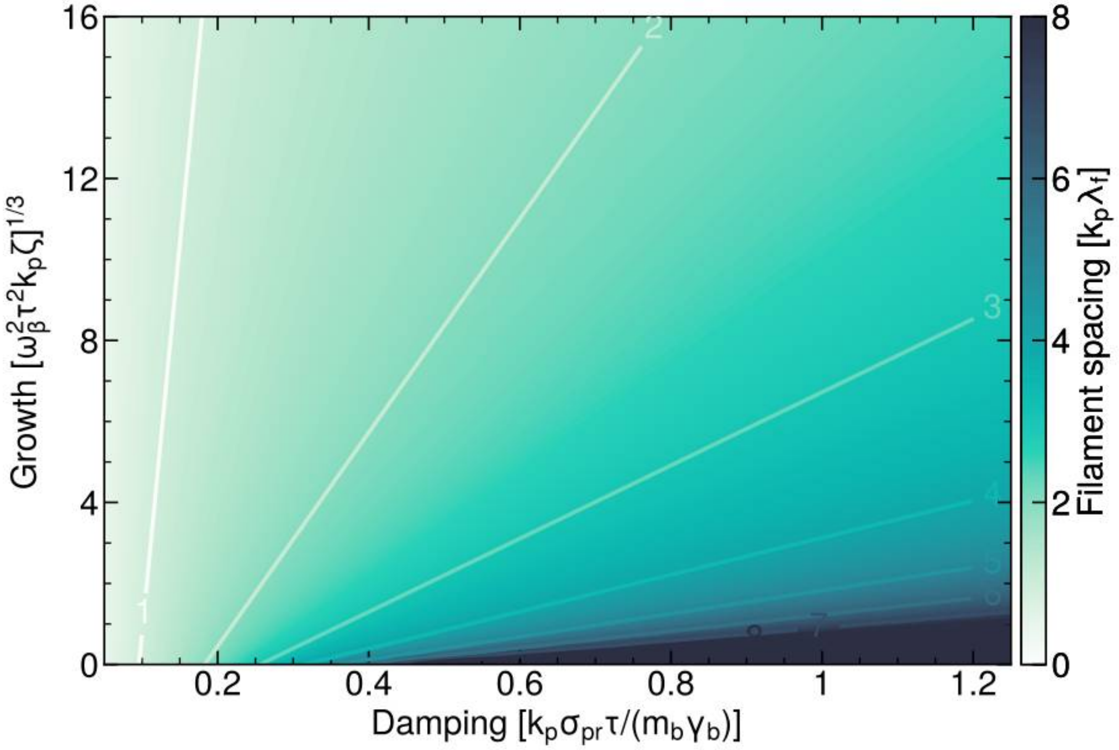

Increase in beam divergence
➤ Filament spacing increases

Experimental Observation of the Filamentation Instability

Expected filament spacing: $\lambda_f = 2\pi / k_{E\max}$
numerically evaluated from

$$1 + 3k_{E_{\max}}^2 + 4N_\infty(k_{E_{\max}}) = 6(1 + k_{E_{\max}}^2)\nu_d(k_{E_{\max}})\tau$$

Increase beam charge
➤ Filament spacing decreases

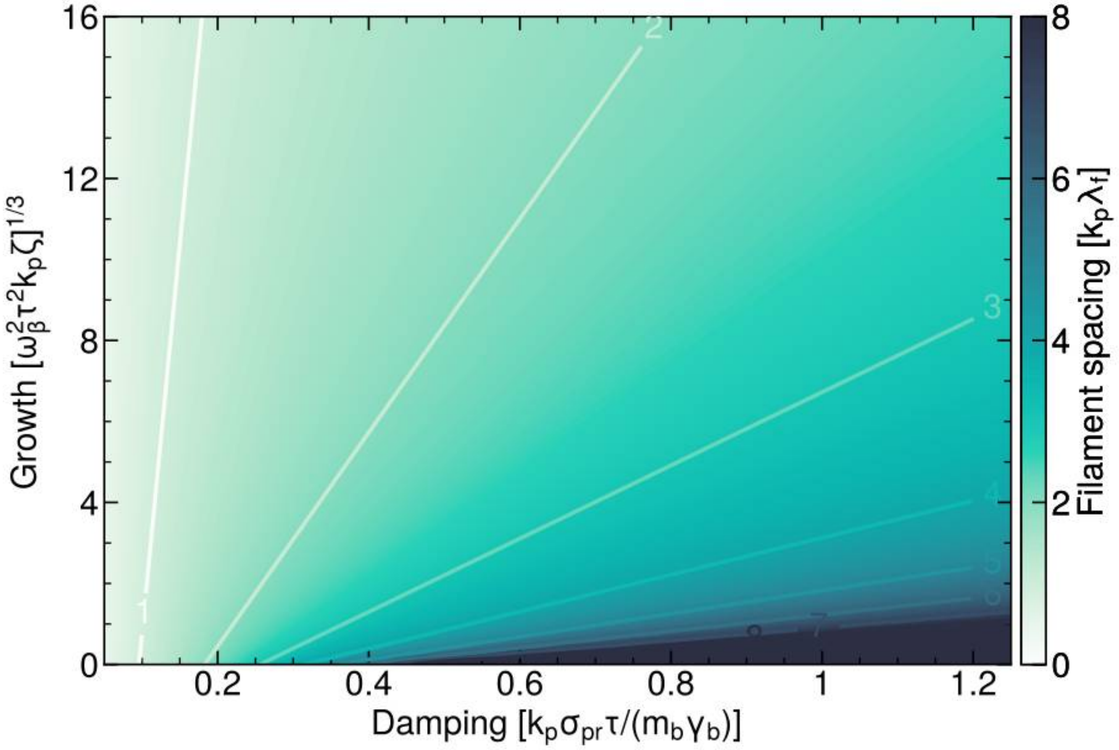

Increase in beam divergence
➤ Filament spacing increases

In Experiment

Parameter	Effect
Increase Focus	Higher beam density and divergence
Increase plasma density	Lower beam density Higher beam length and propagation
Charged beam	**Self-modulating beam**

Experimental Observation of the Filamentation Instability

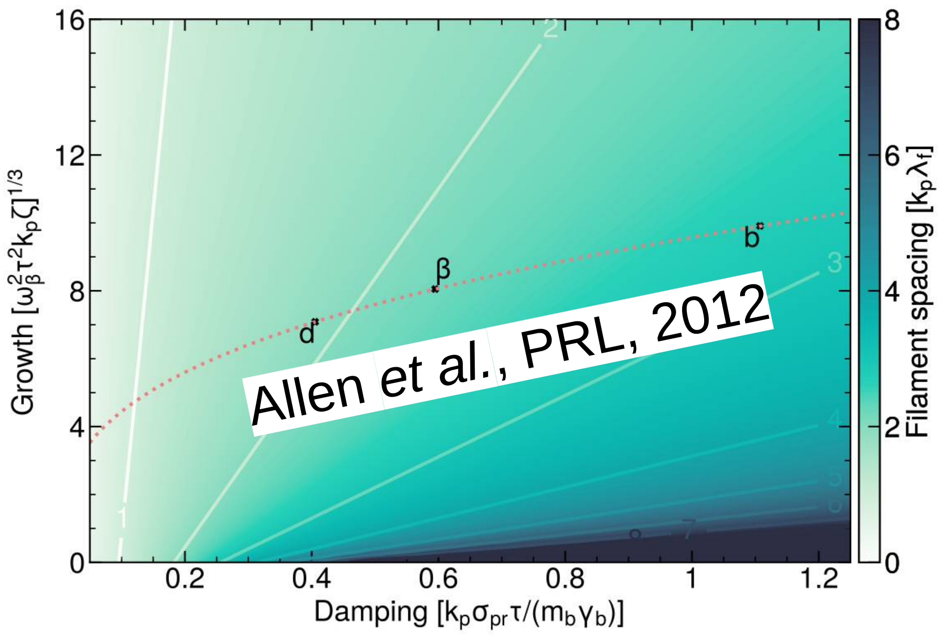

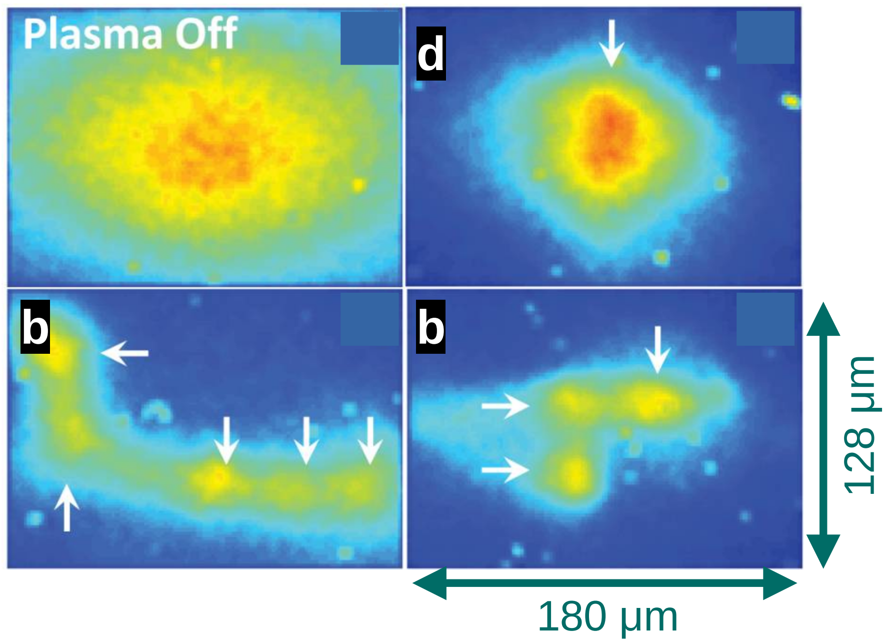

Experimental Observation of the Filamentation Instability

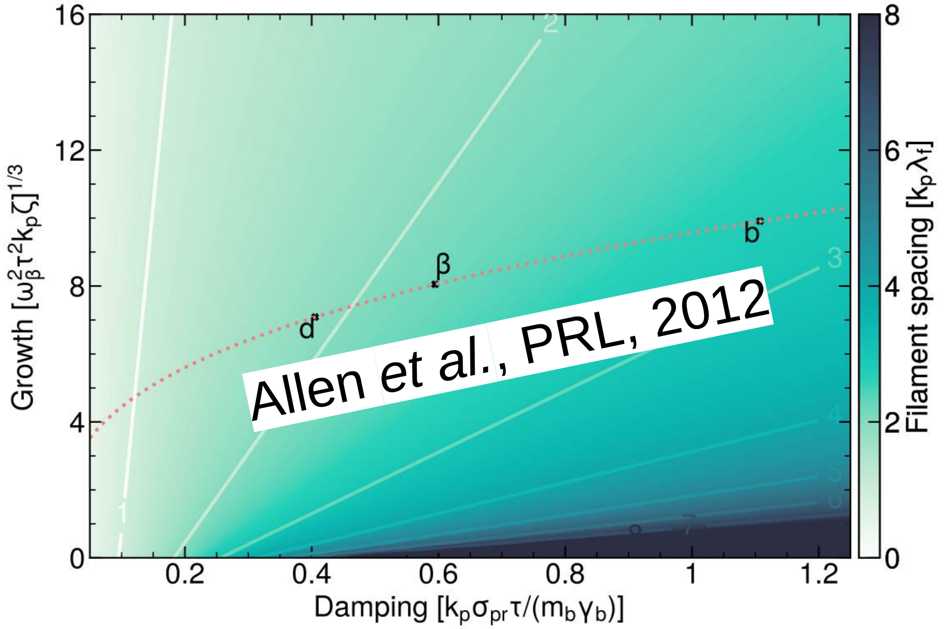

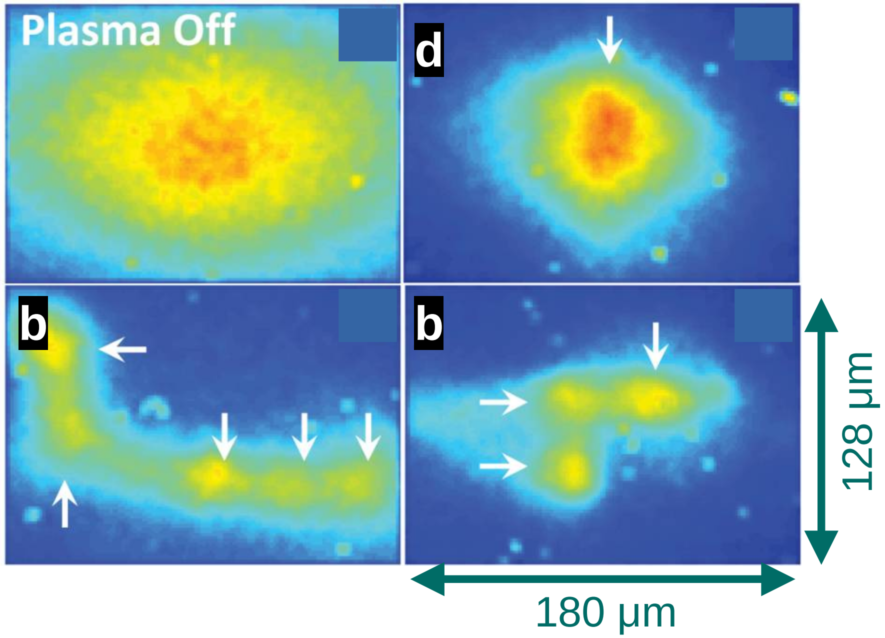

β) $\boldsymbol{\lambda_f=\sigma_r=2.2/k_p}$ @ $3.4\text{x}10^{16}$ cm^{-3}
(filament distance=rms beam width)

b) Filamentation with λ_f=0.042 mm ($12\text{x}10^{16}$ cm^{-3})
d) No filamentation at $1.6\text{x}10^{16}$ cm^{-3}

Experimental Observation of the Filamentation Instability

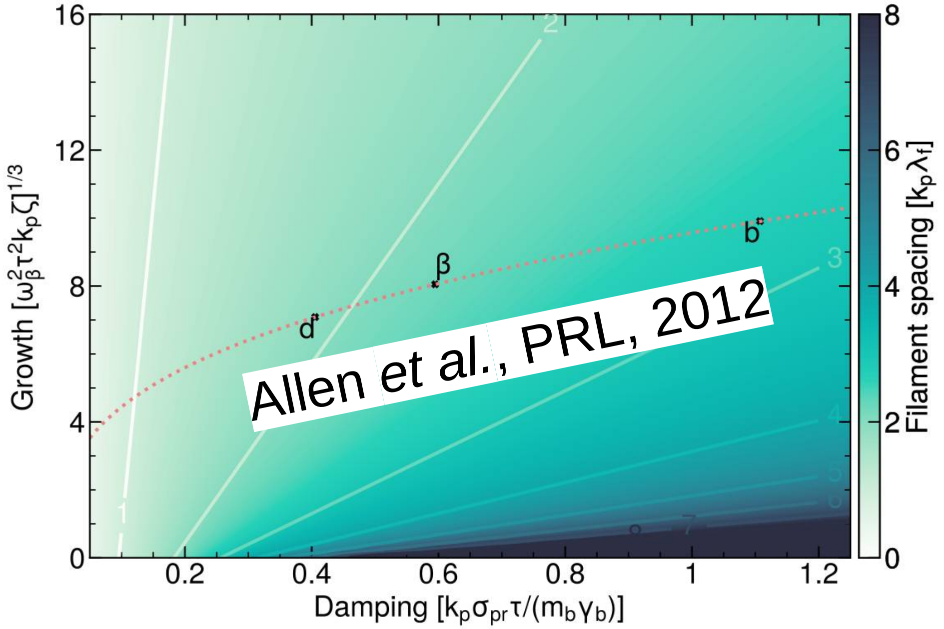

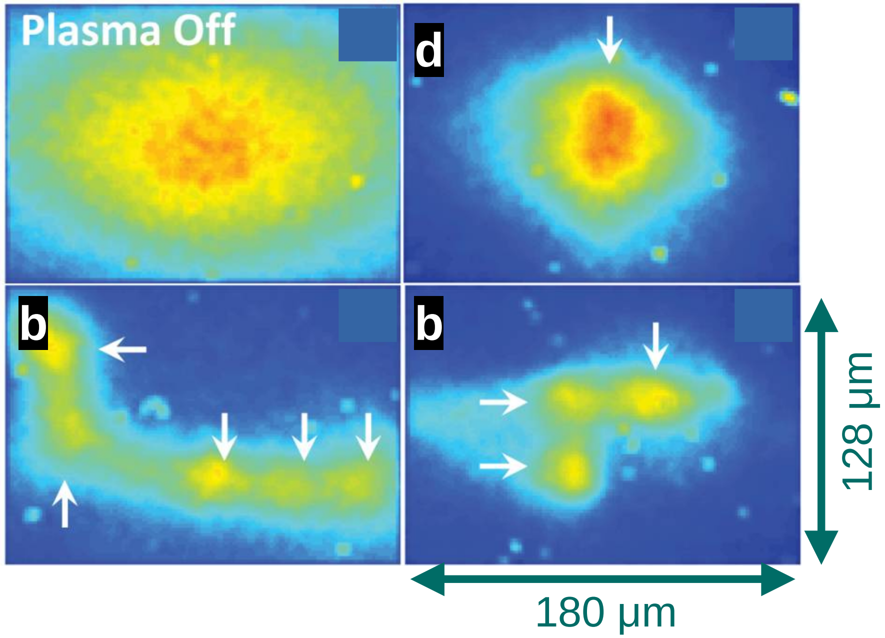

β) **$\lambda_f=\sigma_r=2.2/k_p$** @ 3.4×10^{16} cm^{-3}
(filament distance=rms beam width)

b) Filamentation with λ_f=0.042 mm (12×10^{16} cm^{-3})
d) No filamentation at 1.6×10^{16} cm^{-3}

The agreement to experimental observations undermines the robustness of the analytical model.

Experimental Observation of the Filamentation Instability

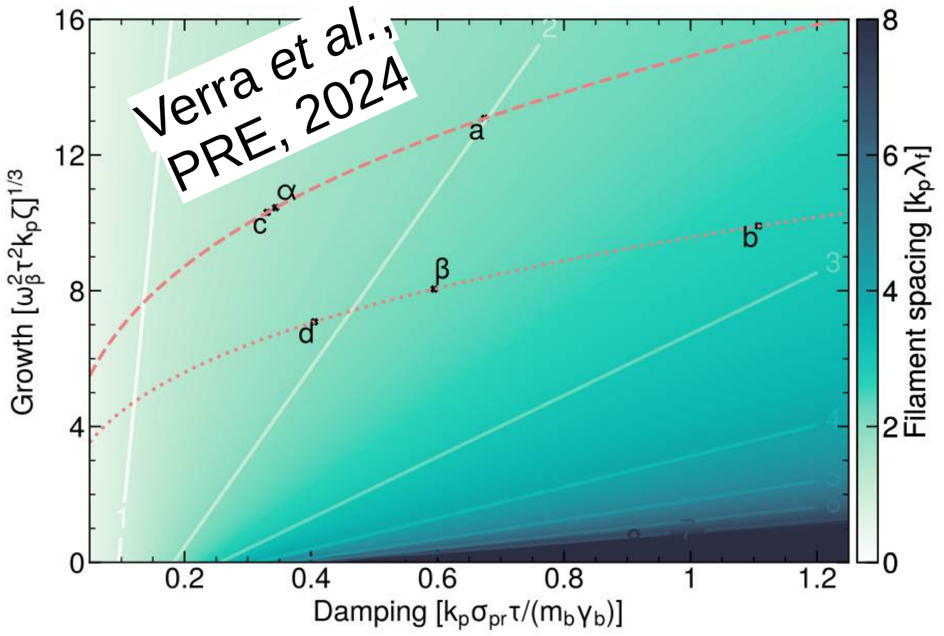

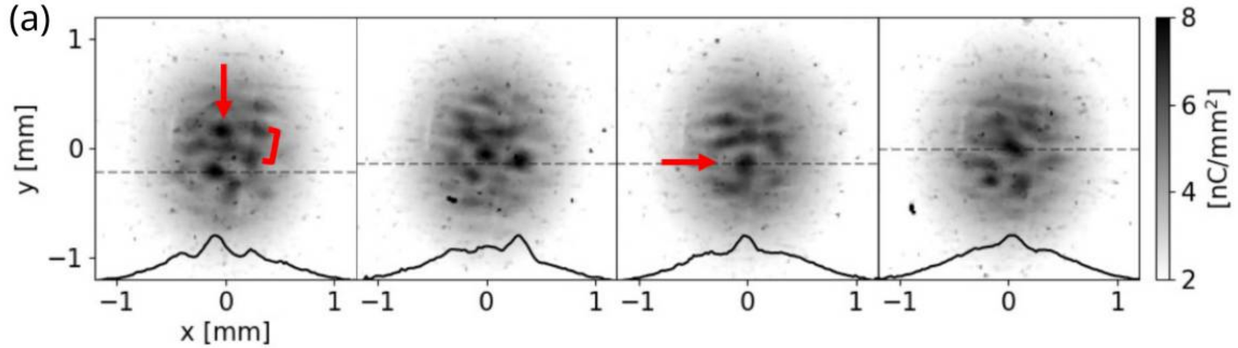

a) Filamentation at n_p=9.38x10^{14} cm^{-3}

λ_f=0.34mm ↔ λ_{exp}=0.33(±0.06) mm

Experimental Observation of the Filamentation Instability

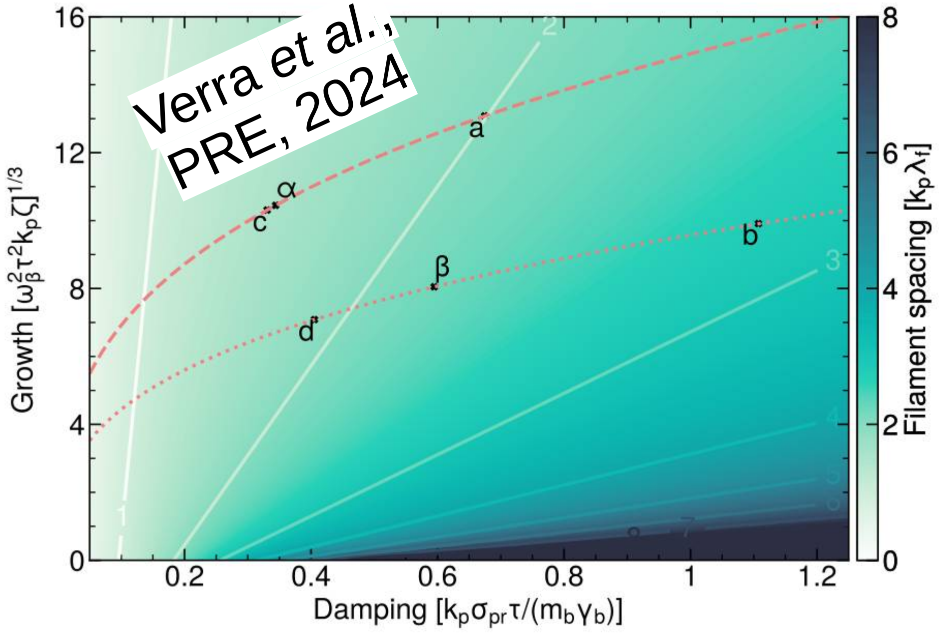

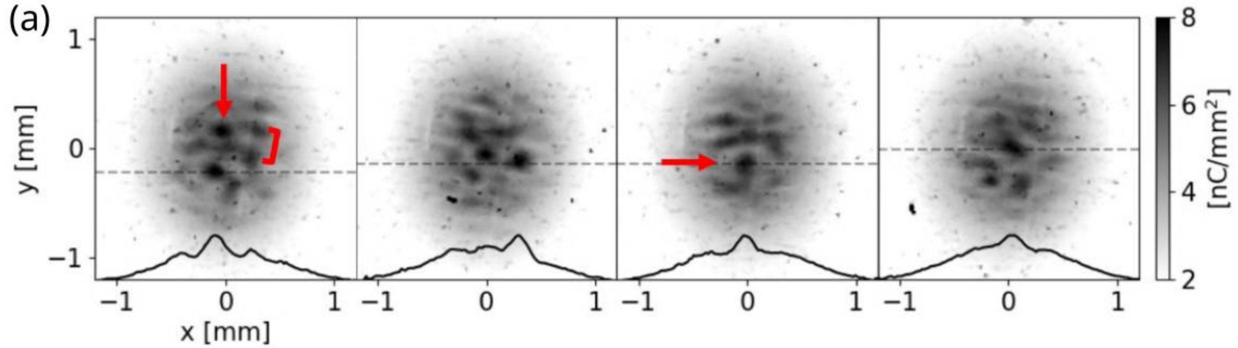

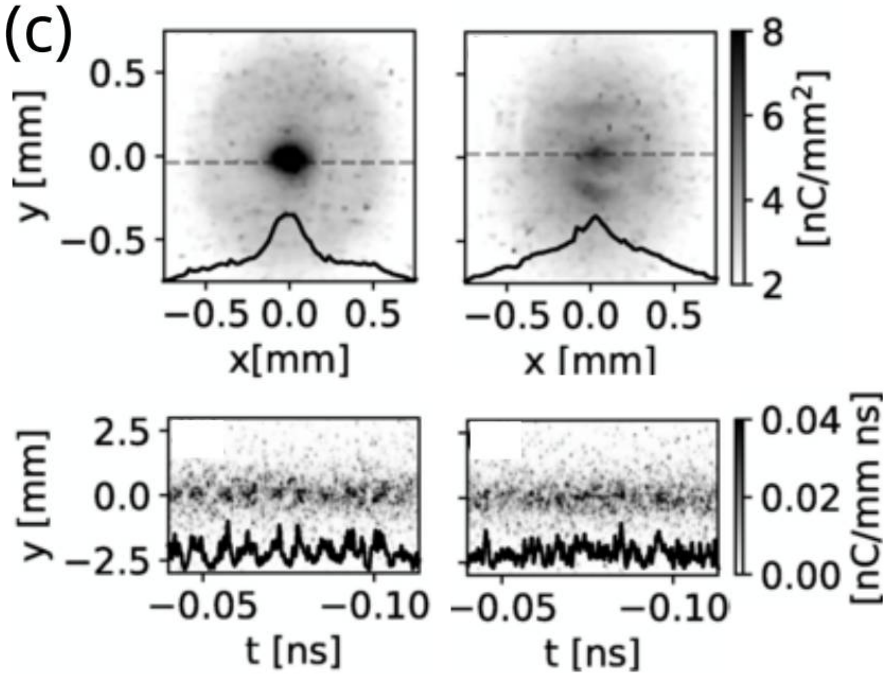

a) Filamentation at n_p=9.38x10^{14} cm^{-3}
λ_f=0.34mm ↔ λ_{exp}=0.33(±0.06) mm

c) n_p=2.25x10^{14} cm^{-3} close to (α) with
λ_f=σ_r=1.5/k_p @ 2.44x10^{14} cm^{-3}

The actual transition between filamentation and self-modulation was shown to occur for
filament spacing = rms beam width

Conclusion

Analytic investigation of wakefield-driven filamentation of finite-sized beams.

- Excellent agreement with simulations and experimental observations

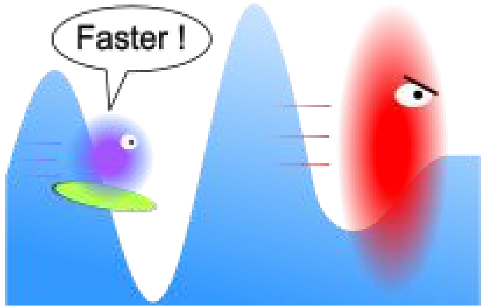

Conclusion

Analytic investigation of wakefield-driven filamentation of finite-sized beams.

- Excellent agreement with simulations and experimental observations

- The growth increases with local transverse density and the longitudinal integrated density
- Diffusion in beams with finite emittance damps small-scale filaments
  → spatiotemporal characteristic wavenumbers.
- Reduced methods (quasistatic, 2D) reproduce fully-electromagnetic, 3D simulations
- Filamentation is suppressed by the self-modulation instability for a filament spacing greater than the beam rms width

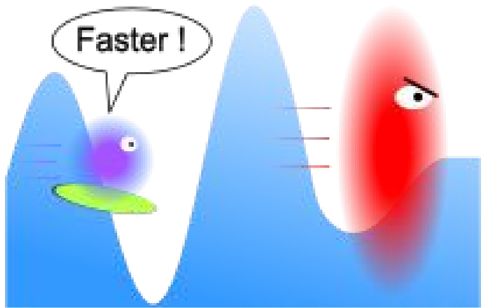

Conclusion

Analytic investigation of wakefield-driven filamentation of finite-sized beams.

- Excellent agreement with simulations and experimental observations

- The growth increases with local transverse density and the longitudinal integrated density
- Diffusion in beams with finite emittance damps small-scale filaments
  →spatiotemporal characteristic wavenumbers.
- Reduced methods (quasistatic, 2D) reproduce fully-electromagnetic, 3D simulations
- Filamentation is suppressed by the self-modulation instability for a filament spacing greater than the beam rms width

These findings provide a crucial basis for designing experiments investigating filamentation and for wakefield accelerator experiments seeking to avoid them.

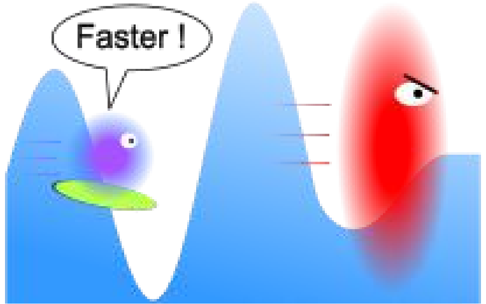

Conclusion

Analytic investigation of wakefield-driven filamentation of finite-sized beams.

➢ Excellent agreement with simulations and experimental observations

- The growth increases with local transverse density and the longitudinal integrated density
- Diffusion in beams with finite emittance damps small-scale filaments
  → spatiotemporal characteristic wavenumbers.
- Reduced methods (quasistatic, 2D) reproduce fully-electromagnetic, 3D simulations
- Filamentation is suppressed by the self-modulation instability for a filament spacing greater than the beam rms width

These findings provide a crucial basis for designing experiments investigating filamentation and for wakefield accelerator experiments seeking to avoid them.

Thank you for your attention!

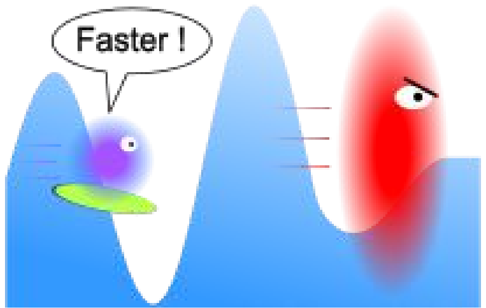

APPENDIX

Experimental Observation of the Filamentation Instability

AWAKE-like wide beam @ 6.4 m

- Spatiotemporal growth of filamentation
- longitudinal modulation at varying phase due to its temperature
- Beam is coarser in simulations
- Growth of envelope agrees with analytical model for TTS

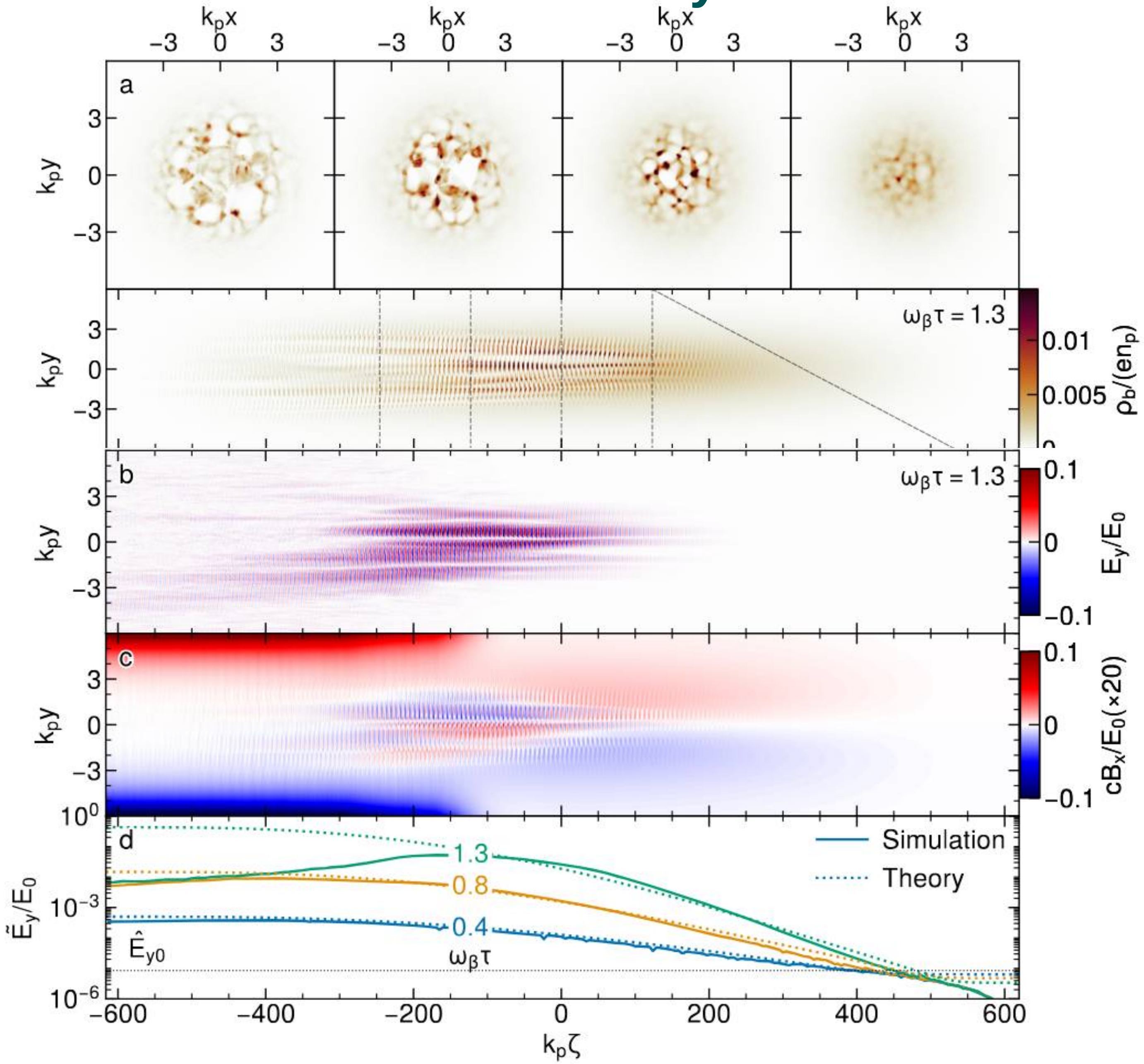

Saturation of Two-Stream Filamentation

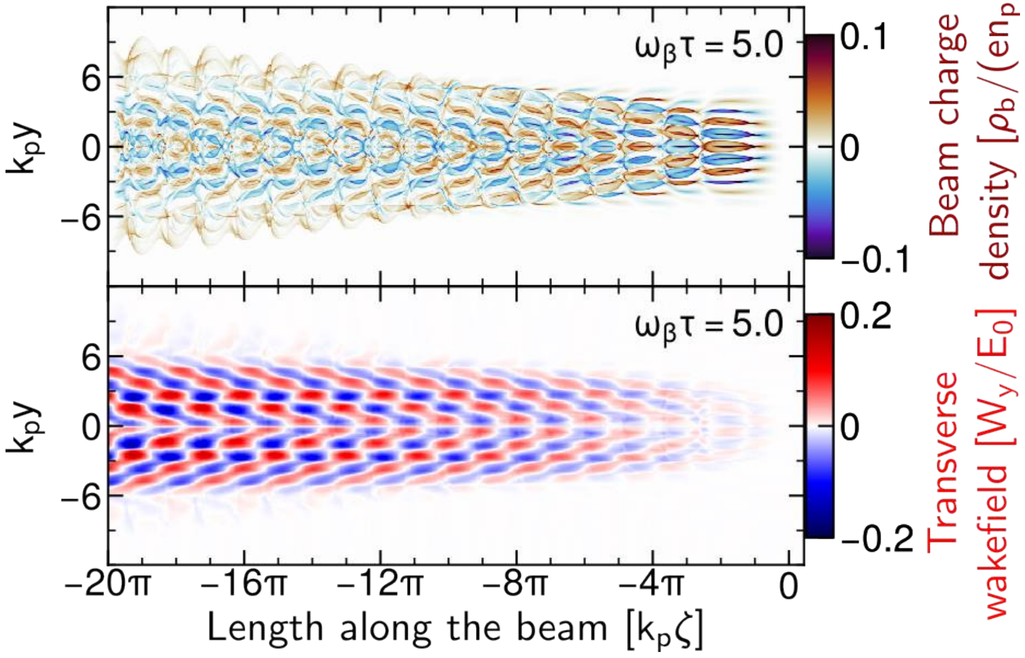

- Filamentation saturates for $\delta n_{b,p} \approx n_{b,p}$
- Beam and filaments diverge

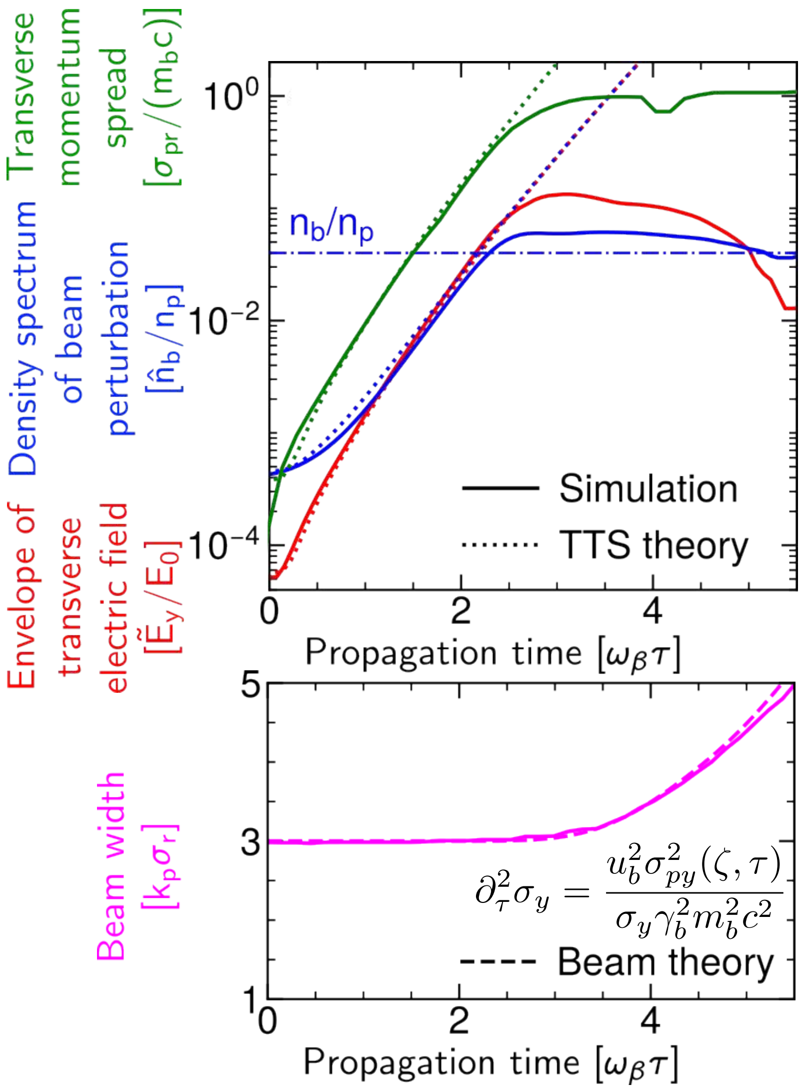

Momentum spread grows with transverse wakefield

Particles detrap under high momentum spread and the rms width increases as the wakefield saturates

Ion Motion in Wakefield-driven Instabilities

Ponderomotive force of wakefield envelope acts on heavy ions

- Non-homogeneous ion background

Detuning from the resonant condition

- Transverse wavebreaking
  (Minakov&Lotov, 2024; Vieira *et al.*, 2014)
- Transverse decoherence
  (Turner *et al.* AWAKE Collab., 2024)
- Detuning of the wakefield from the microbunches

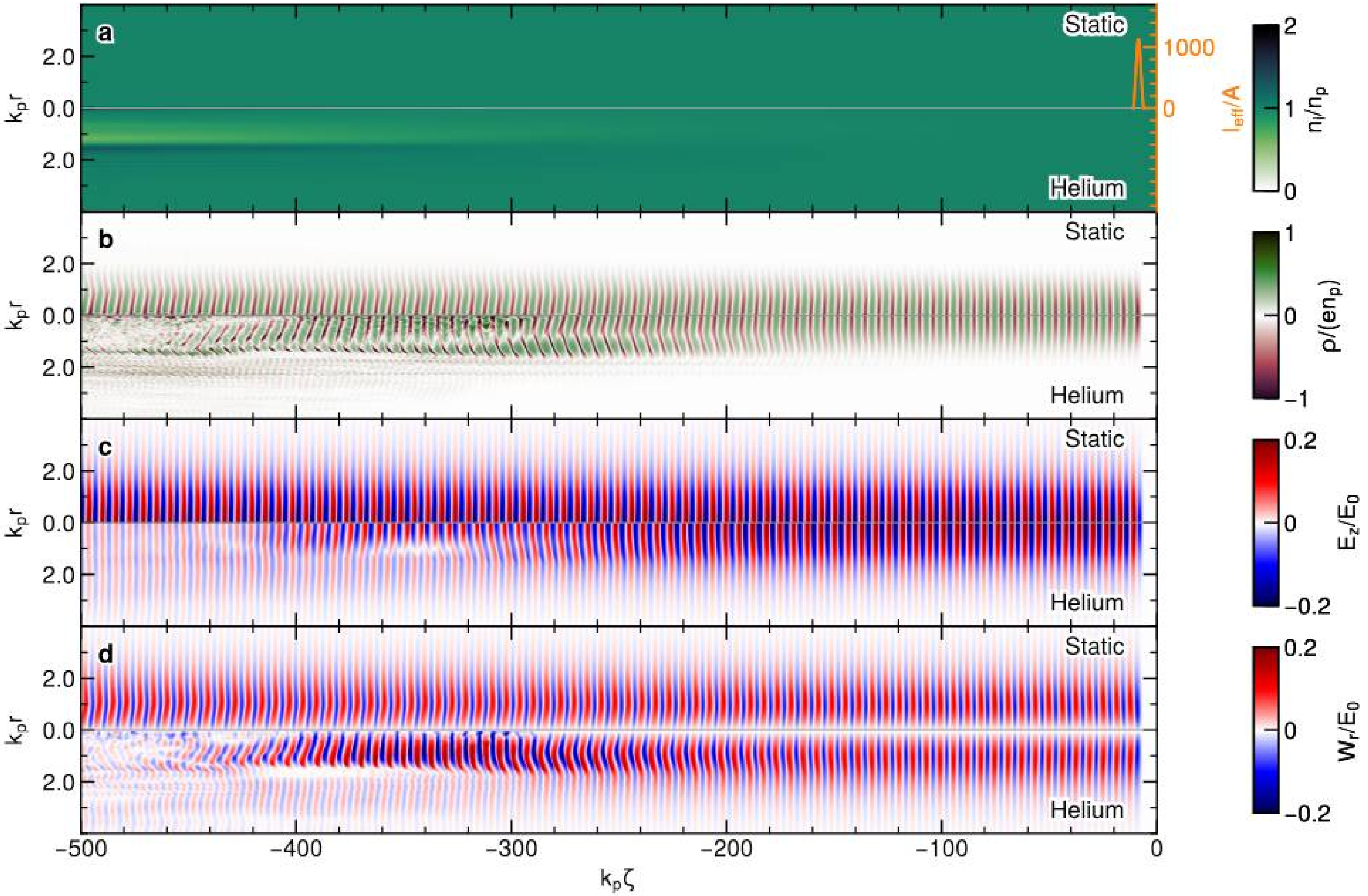

Ion Motion in Wakefield-driven Instabilities

Collective transverse motion of plasma electrons is disturbed by non-local plasma wavelength

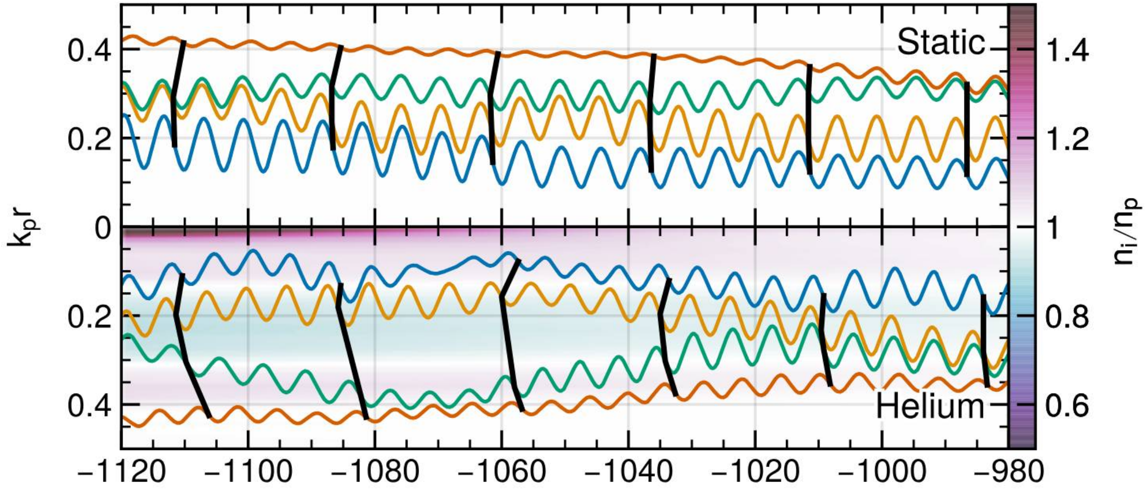

Cumulative effect on the SMI

- Beam tail weakly modulated as radial wakefield decreases
- Beam head shorter due to the detuning wakefield

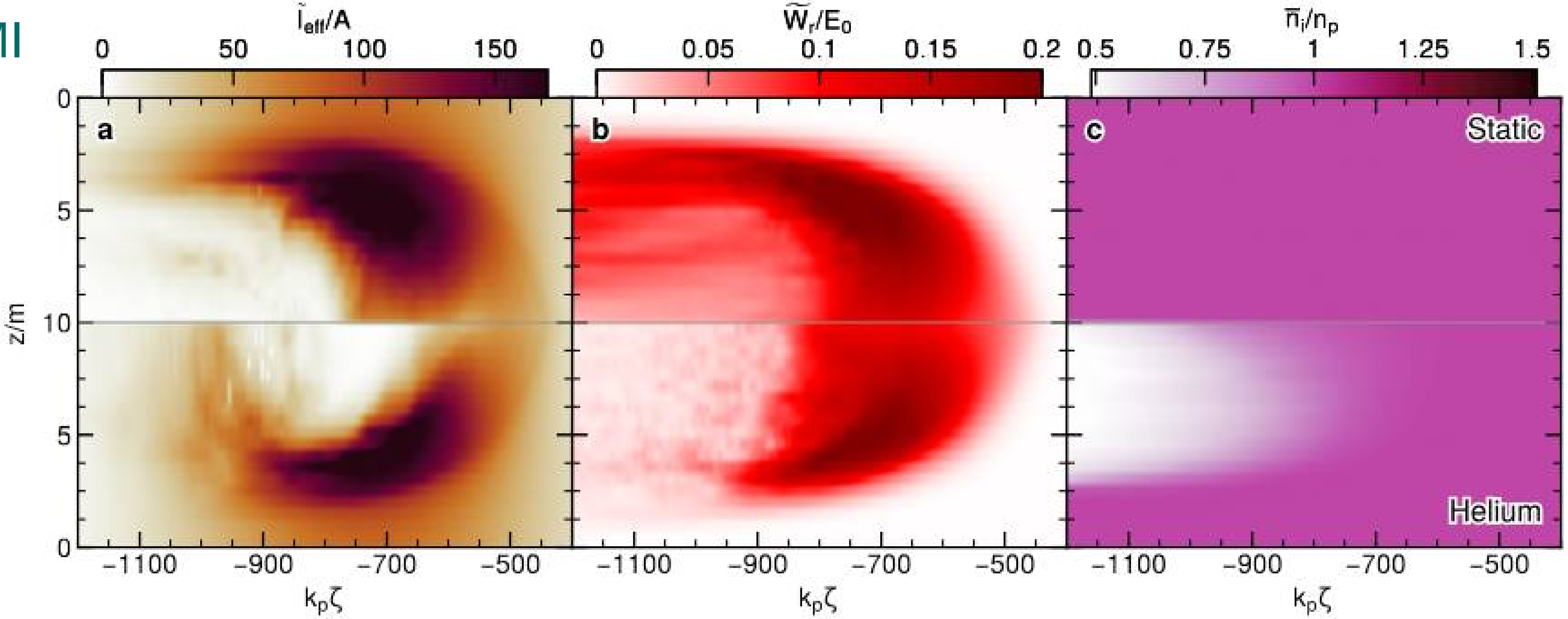

Ion Motion in Wakefield-driven Instabilities

Effect of ion motion on wakefield-driven filamentation comparable to SMI

- Wakefield reduces in non-linear stage of TTS

Ion motion enhances electromagnetic field due to secondary ion CFI

- Ion filaments pervade beyond the beam

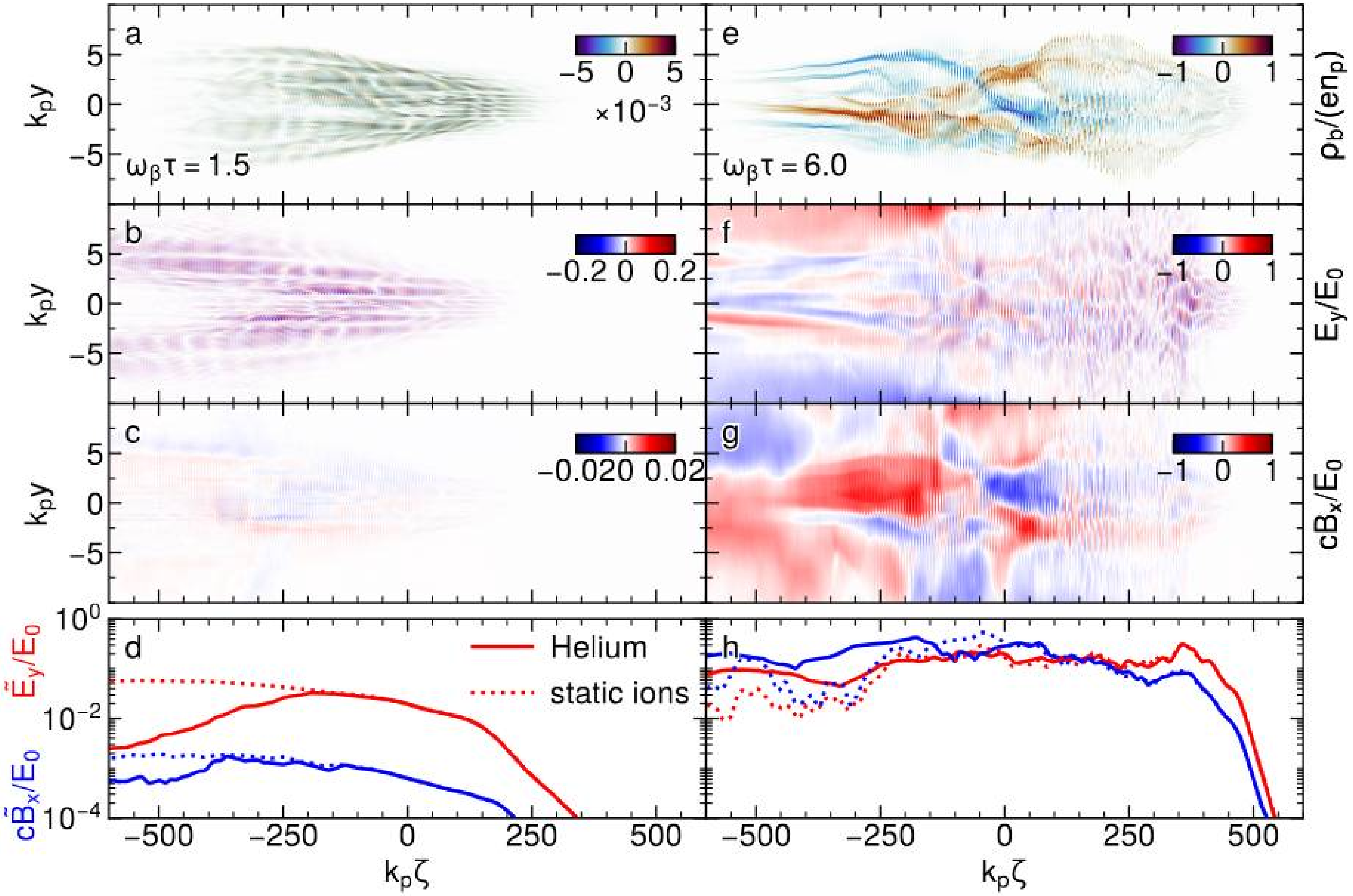

Transition between Filamentation Instabilities

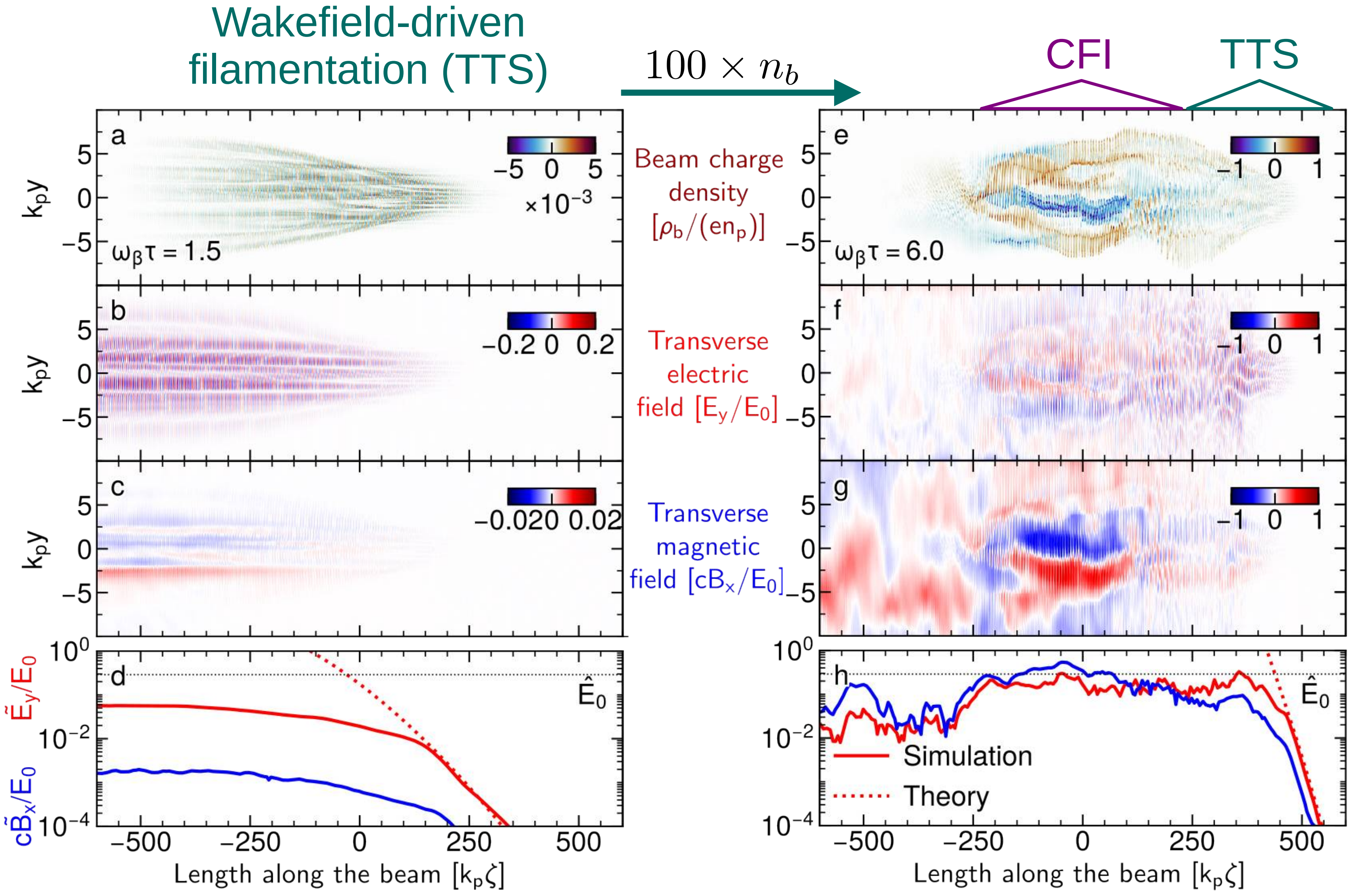

Beam head: Driven by wakefield

Towards beam center:

- Wakefield saturates ($\delta n_p \approx n_p$)
- Particles bunch together with weaker long. modulation
- Growing magnetic field dominates

For dense beams, the wakefield sets the initial condition for CFI at the beam center.

Derivation of Wakefield-Driven Filamentation

Ansatz: Fourier transform of **wave equations**

$$(\nabla^2 - \partial_t^2/c^2)\mathbf{E} = \mu_0 \partial_t \mathbf{j} + \nabla\rho/\varepsilon_0$$
$$(\nabla^2 - \partial_t^2/c^2)\mathbf{B} = -\mu_0 \nabla \times \mathbf{j}$$

- Dilute beam
- Relativistic beam with $\omega_\beta << \omega_p$

$$\mu_0 \partial_t j_p = -k_p^2 E$$
$$(\partial_z^2 - \partial_t^2/c^2)\delta\rho_p \rightarrow \partial_\zeta^2 \delta\rho_p/\gamma_b^2 \text{ as } |\partial_\zeta \delta\rho_p| \gg |\partial_\tau \delta\rho_p / u_b|$$

In linear theory, the wakefield spectrum only depends on the beam charge density

$$\hat{E}_z = -\frac{}{\varepsilon_0\sqrt{2\pi}} \frac{k_\zeta (k_\zeta^2/\gamma_b^2 + k_p^2)\mathcal{F}_{\zeta xy}\{\rho_b\}}{(k_\zeta^2 - k_e^2)(k_\zeta^2/\gamma_b^2 + k_p^2 + k_r^2)}$$

$$\hat{E}_\perp = \frac{1}{\varepsilon_0\sqrt{2\pi}} \frac{k_\zeta^2 \mathcal{F}_{\zeta xy}\{\nabla_\perp \rho_b\}}{(k_\zeta^2 - k_e^2)(k_\zeta^2/\gamma_b^2 + k_p^2 + k_r^2)}$$

$$\hat{B}_\perp = \frac{u_b/c^2}{\varepsilon_0\sqrt{2\pi}} \frac{\mathcal{F}_{\zeta xy}\{\nabla^\perp \rho_b\}}{k_\zeta^2/\gamma_b^2 + k_p^2 + k_r^2},$$

Derivation of Wakefield-Driven Filamentation

Inverse Fourier transform for charge density with **transverse modulation**

$$\rho_{b0} = q_b \delta n_{b0} f(\zeta) g(x,y)$$
$$g(x,y) = \tilde{g}(x,y) \cos\left(k_x x + \varphi_x\right) \cos\left(k_y y + \varphi_y\right)$$

- For wide beams, spectral broadening due to envelope is negligible

$$E_\perp \sim \mathcal{F}_{xy}^{-1}\left\{\frac{\mathcal{F}_{xy}\left\{\nabla_\perp g(x,y)\right\}}{k_e^2 + k_r^2}\right\} \approx \frac{\nabla_\perp g(x,y)}{k_e^2 + k_r^2}$$

Electromagnetic field in plasma excited by the beam

Plasma Wakefield

$$E_z = \frac{q_b \delta n_b}{\varepsilon_0} \frac{k_e g(x,y)}{k_e^2 + k_r^2} \boxed{\int_\zeta^0 \mathrm{d}\zeta' f(\zeta') k_e \cos k_e(\zeta - \zeta')}$$
$$\mathbf{E}_\perp = \frac{q_b \delta n_b}{\varepsilon_0} \frac{\nabla_\perp g(x,y)}{k_e^2 + k_r^2} \left[\boxed{\int_\zeta^0 \mathrm{d}\zeta' f(\zeta') k_e \sin k_e(\zeta - \zeta')} - \boxed{f(\zeta)}\right]$$
$$\mathbf{B}_\perp = -\frac{u_b}{c^2} \frac{q_b \delta n_b}{\varepsilon_0} \frac{\nabla^\perp g(x,y)}{k_p^2 + k_r^2} \boxed{f(\zeta)}.$$

Beam self-fields

Simulating Filamentation

Methods to mitigate numerical instabilities

- Fei EM-field solver (avoids numerical Cherenkov)
- 5-pass compensated binomial current filter
- Load particles with different opposite charge at identical positions (avoids fringe fields)

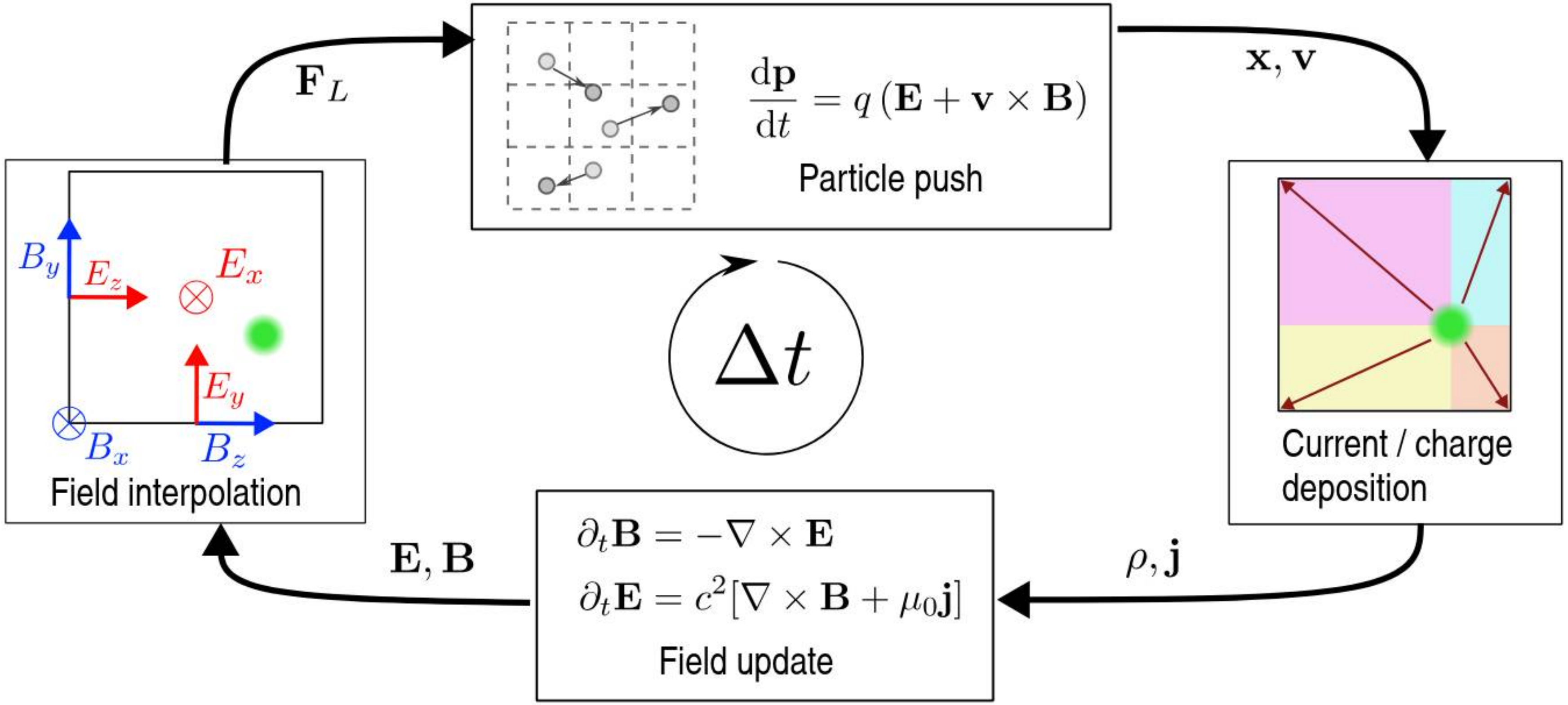

Simulating Filamentation

Beam filamentation commonly simulated with electromagnetic codes

- 2 relevant modes in a relativistic, neutral (e+e-) bunch (based on *Shukla, 2018*)

Current filamentation instability

- Dominant magnetic field (*Shukla, 2018*)
- Saturation: Magnetic trapping & filaments merge (R.C. Davidson, 1972)

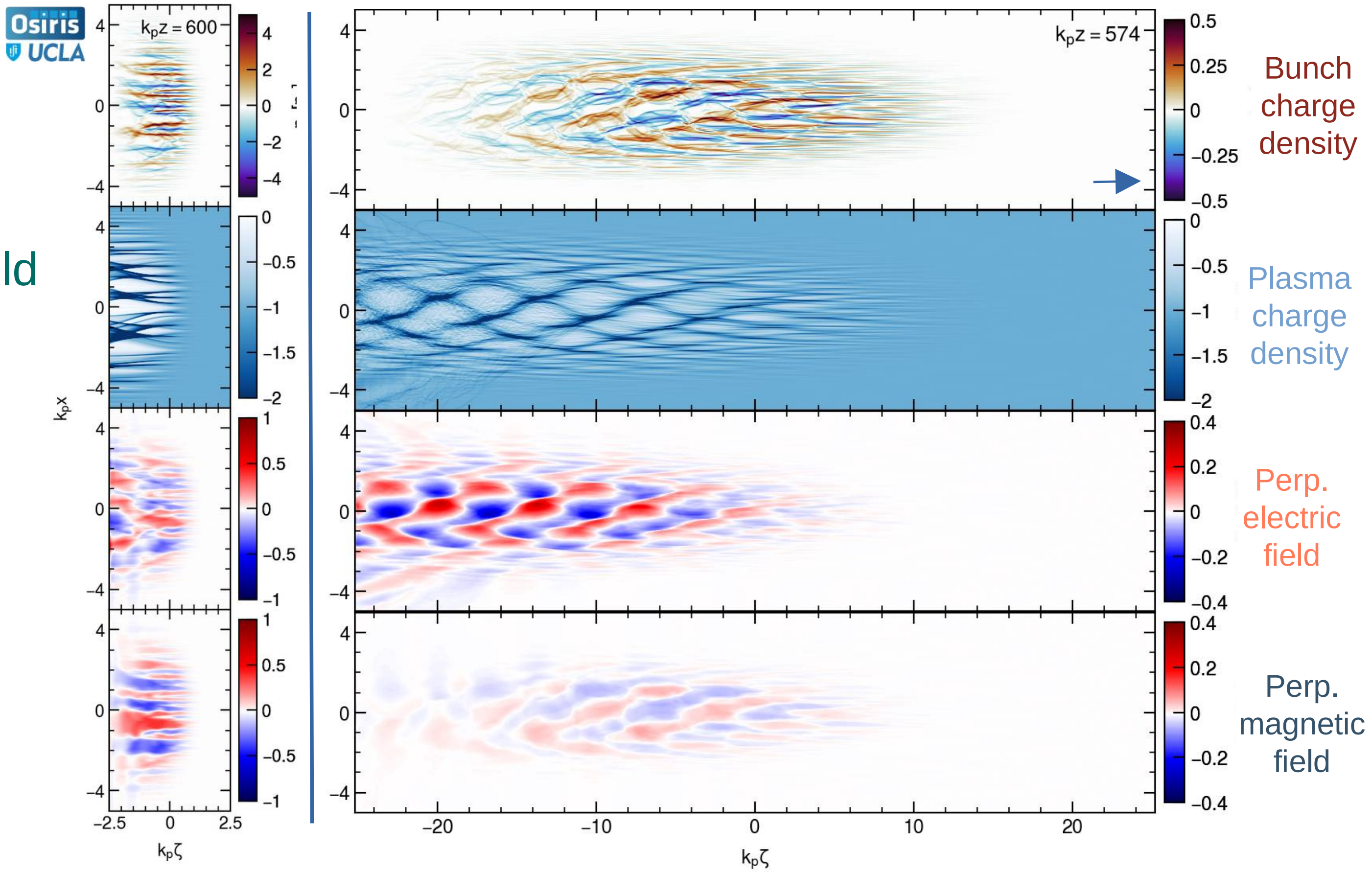

Oblique instability

- Transvers + longitudinal mode (*A. Bret, 2010*)
- Particles motion governed by electric field